

S-matrix equivalence restored

Chih-Hao Fu,[†] Jonathan Fudger,[‡] Paul R.W. Mansfield,[†] Tim R. Morris[‡] and Zhiguang Xiao[‡]

[†]*Department of Mathematical Sciences, University of Durham
South Road, Durham, DH1 3LE, U.K.*

[‡]*School of Physics and Astronomy, University of Southampton
Highfield, Southampton, SO17 1BJ, U.K.*

*E-mails: chih-hao.fu@durham.ac.uk, j.p.fudger@phys.soton.ac.uk,
P.R.W.Mansfield@durham.ac.uk, T.R.Morris@soton.ac.uk,
z.g.xiao@phys.soton.ac.uk*

ABSTRACT: The canonical transformation that maps light-cone Yang-Mills theory to a Lagrangian description of the MHV rules is non-local, consequently the two sets of fields do not necessarily generate the same S-matrix. By deriving a new recursion relation for the canonical transformation expansion coefficients, we find a direct map between these coefficients and tree level light-cone diagrams. We use this to show that, at least up to one-loop with dimensionally regularised MHV vertices, the only difference is the omission of the one-loop amplitudes in which all gluons have positive helicity.

KEYWORDS: Gauge symmetry, QCD.

Contents

1. Introduction	1
2. Dimensional Regularisation	5
3. Canonical transformation in D dimensions	6
3.1 Recursion relations for the expansion coefficients	6
3.2 Reconstructing the expansion coefficients from tree-level light-cone diagrams	11
4. ‘Missing’ amplitudes from equivalence theorem evasion reviewed	12
5. Equivalence theorem evasion in general.	14
5.1 Tree-level	15
5.2 One loop	17
5.2.1 Dressing propagators	17
5.2.2 Tadpoles	19
5.2.3 Infra-red divergent loop integration	20
6. One-loop $(- + ++)$ amplitude	22
7. One-loop $(+ + -)$ amplitude with external tadpole dressing propagators	23
8. Conclusion and higher loops	25
A. Some remaining thoughts on translation kernels	27
B. Proof of recursion relation (3.9)	32

1. Introduction

The MHV rules of Cachazo, Svrček and Witten [1] are equivalent to a new set of Feynman rules for QCD tree-level scattering amplitudes that are particularly efficient. Initially conjectured on the basis of an analogy with strings moving on twistor space [2] they were proven by recursion relations [3]. They emerge from gauge fixing a twistor space action for Yang-Mills [4]-[10] and can also be derived using a canonical transformation applied to the light-cone gauge Yang-Mills Lagrangian [11, 12]. To generalise these rules to loop level requires the introduction of a regulator, for example some variant of dimensional regularisation. Although much of the mathematical structure underlying this approach to Yang-Mills theory, such as conformal invariance and twistor space, is broken by the passage to arbitrary dimension there is some cause for optimism that progress towards formulating

MHV rules for loop processes can still be made [13]. One of the features that emerges at loop order is that the new fields do not generate the same S-matrix as the original ones because of the non-locality of the canonical transformation. This effect accounts for the one-loop amplitudes for gluons of purely positive helicity which would otherwise appear to be absent from the theory. However, it is potentially damaging for the efficiency of the MHV rules because it would seem to require an extra ingredient in the calculation of amplitudes to describe the translation between the two sets of fields. It is the purpose of this paper to show that although extra structure is required to translate between the two sets of fields, these ‘translation kernels’ are required only for all plus amplitudes at one-loop, so that for the calculation of general amplitudes we are free to use Green functions for either set of fields, thus partially regaining the simplicity of the CSW rules for the regulated theory. In theories with exact supersymmetry these problems are absent and it is known that four dimensional MHV vertices and MHV rules may be used to recover all amplitudes at one loop [26].

We begin by describing the canonical transformation as it is constructed in four dimensions. Using light-cone co-ordinates in Minkowski space

$$\hat{x} = \frac{1}{\sqrt{2}}(t - x^3), \quad \tilde{x} = \frac{1}{\sqrt{2}}(t + x^3), \quad z = \frac{1}{\sqrt{2}}(x^1 + ix^2), \quad \bar{z} = \frac{1}{\sqrt{2}}(x^1 - ix^2). \quad (1.1)$$

and the gauge condition $\hat{A} = 0$ allows the Yang-Mills action to be written in terms of positive and negative helicity fields $\mathcal{A} \equiv A_z$ and $\bar{\mathcal{A}} \equiv A_{\bar{z}}$ (after elimination of unphysical degrees of freedom) as the light-cone action

$$S = \frac{4}{g^2} \int d\hat{x} \int_{\Sigma} d^3\mathbf{x} (\mathcal{L}^{-+} + \mathcal{L}^{-++} + \mathcal{L}^{--+} + \mathcal{L}'^{--+}), \quad (1.2)$$

where

$$\mathcal{L}^{-+} = \text{tr } \bar{\mathcal{A}} \left(\hat{\partial} \hat{\partial} - \partial \bar{\partial} \right) \mathcal{A}, \quad (1.3)$$

$$\mathcal{L}^{-++} = -\text{tr} (\bar{\partial} \hat{\partial}^{-1} \mathcal{A}) [\mathcal{A}, \hat{\partial} \bar{\mathcal{A}}], \quad (1.4)$$

$$\mathcal{L}^{--+} = -\text{tr} [\bar{\mathcal{A}}, \hat{\partial} \mathcal{A}] (\partial \hat{\partial}^{-1} \bar{\mathcal{A}}), \quad (1.5)$$

$$\mathcal{L}'^{--+} = -\text{tr} [\bar{\mathcal{A}}, \hat{\partial} \mathcal{A}] \hat{\partial}^{-2} [\mathcal{A}, \hat{\partial} \bar{\mathcal{A}}], \quad (1.6)$$

and Σ is a constant- \hat{x} quantisation surface and $d^3\mathbf{x} = d\tilde{x} dz d\bar{z}$.

The combination $\mathcal{L}^{-+} + \mathcal{L}^{-++}$ by itself describes self-dual gauge theory [14]. At tree-level this is a free theory because the only connected scattering amplitudes that can be constructed involve one negative helicity particle and an arbitrary number of positive helicity particles. The Feynman diagrams contributing to this are the same as in the full Yang-Mills theory, for which such amplitudes are known to vanish. (Bizarrely, the one-loop amplitudes for processes involving only positive helicity particles are non-zero, and these are the only non-vanishing amplitudes in the theory.) This encourages us to find a new field \mathcal{B} that is a non-local functional of \mathcal{A} on the surface of constant \hat{x} such that $\mathcal{L}^{-+} + \mathcal{L}^{-++}$ can be written as a free theory, i.e.

$$\mathcal{L}^{-+}[\mathcal{A}, \bar{\mathcal{A}}] + \mathcal{L}^{-++}[\mathcal{A}, \bar{\mathcal{A}}] = \mathcal{L}^{-+}[\mathcal{B}, \bar{\mathcal{B}}], \quad (1.7)$$

where $\bar{\mathcal{B}}$ is determined by the requirement that the transformation be canonical:

$$\hat{\partial}\bar{\mathcal{A}}^a(\hat{x}, \mathbf{x}) = \int_{\Sigma} d^3\mathbf{y} \frac{\delta\mathcal{B}^b(\hat{x}, \mathbf{y})}{\delta\mathcal{A}^a(\hat{x}, \mathbf{x})} \hat{\partial}\bar{\mathcal{B}}^b(\hat{x}, \mathbf{y}) \Leftrightarrow \hat{\partial}\bar{\mathcal{B}}^a(\hat{x}, \mathbf{x}) = \int_{\Sigma} d^3\mathbf{y} \frac{\delta\mathcal{A}^b(\hat{x}, \mathbf{y})}{\delta\mathcal{B}^a(\hat{x}, \mathbf{x})} \hat{\partial}\bar{\mathcal{A}}^b(\hat{x}, \mathbf{y}). \quad (1.8)$$

This transformation is readily expressed in terms of the fields after taking the Fourier transform with respect to position within the quantisation surface

$$\mathcal{B}(\hat{x}, \mathbf{p}) = \mathcal{A}(\hat{x}, \mathbf{p}) + \sum_{n=2}^{\infty} \int \frac{d^3k_1}{(2\pi)^3} \cdots \frac{d^3k_n}{(2\pi)^3} \frac{\hat{p}^{n-1} (2\pi)^3 \delta^3(\mathbf{p} - \sum \mathbf{k}_i)}{(p, k_1)(p, k_1 + k_2) \dots (p, k_1 + \dots + k_{n-1})} \mathcal{A}(\hat{x}, \mathbf{k}_1) \dots \mathcal{A}(\hat{x}, \mathbf{k}_n) \quad (1.9)$$

where

$$(k_1, k_2) \equiv \hat{k}_1 k_2 - \hat{k}_2 k_1. \quad (1.10)$$

The transformation is therefore local in \hat{x} and the coefficients of the products $\mathcal{A} \dots \mathcal{A}$ are independent of both \hat{x} and \bar{k} . (1.8) shows that $\bar{\mathcal{A}}$ is a linear functional of $\bar{\mathcal{B}}$, which we write as

$$\begin{aligned} \bar{\mathcal{A}}(\hat{x}, \mathbf{p}) = & \bar{\mathcal{B}}(\hat{x}, \mathbf{p}) + \\ & \sum_{m=3}^{\infty} \sum_{s=2}^m \int \frac{d^3k_1}{(2\pi)^3} \cdots \frac{d^3k_n}{(2\pi)^3} \frac{\hat{k}_s}{\hat{p}} \Xi^{s-1}(\mathbf{p}, -\mathbf{k}_1, \dots, -\mathbf{k}_m) \times \\ & (2\pi)^3 \delta^3(\mathbf{p} - \sum \mathbf{k}_i) \mathcal{B}(\hat{x}, \mathbf{k}_1) \dots \bar{\mathcal{B}}(\hat{x}, \mathbf{k}_s) \dots \mathcal{B}(\hat{x}, \mathbf{k}_m) \end{aligned} \quad (1.11)$$

so that when the remaining terms in the action are written in the new variables we obtain an infinite series, each term of which contains two powers of $\bar{\mathcal{B}}$. Labelling these terms by their helicities gives

$$\mathcal{L}[\mathcal{A}, \bar{\mathcal{A}}] = \mathcal{L}^{-+}[\mathcal{B}, \bar{\mathcal{B}}] + \mathcal{L}^{--}[\mathcal{B}, \bar{\mathcal{B}}] + \mathcal{L}^{-++}[\mathcal{B}, \bar{\mathcal{B}}] + \mathcal{L}^{--++}[\mathcal{B}, \bar{\mathcal{B}}] + \dots \quad (1.12)$$

The coefficients of the fields in the interaction terms can be shown [16], by explicit calculation, to consist of the Parke-Taylor amplitudes [17] (continued off-shell).

The LSZ procedure gives scattering amplitudes in terms of the momentum space Green functions (suitably normalised) for \mathcal{A} and $\bar{\mathcal{A}}$ fields by cancelling each external leg using a factor p^2 and then taking each momentum on-shell, $p^2 \rightarrow 0$. The equivalence theorem for S-matrix elements seems to allow us to use Green functions for the \mathcal{B} and $\bar{\mathcal{B}}$ fields instead of the \mathcal{A} and $\bar{\mathcal{A}}$, provided we include a multiplicative wave-function renormalisation. This is because, to leading order in the fields, \mathcal{A} is the same as \mathcal{B} . In any Feynman diagram contributing to a Green function these fields are attached to the rest of the diagram by a propagator $\sim 1/p^2$ which cancels the LSZ factor of p^2 and so survives the on-shell limit. In the higher order terms in (1.9) the momentum p is shared between the \mathcal{A} fields, so the propagators that attach these to diagrams cannot directly cancel p^2 . The cancellation can occur if the diagram forces just these momenta to flow together through some internal line, because by momentum conservation this line will contribute $\sim 1/p^2$. The effect of such diagrams is to renormalise the field, and this will cancel in the computation of scattering

amplitudes. Another source of $1/p^2$ could be the kernels in (1.9). These kernels are non-local within the quantisation surface, and a requirement of the equivalence theorem is that the transformation be local. However our transformation is still local in light-cone ‘time’ \hat{x} which means that the kernels are independent of \tilde{p} (and also, for other reasons, \bar{p}) so it is hard (but not impossible, as we will see) to imagine how the kernels can generate the $1/p^2$ needed to stop us generalising the theorem to the case in hand.

So it would seem safe to invoke the S-matrix equivalence theorem and use the \mathcal{B} fields to calculate scattering amplitudes, expecting to get physical gluon amplitudes. It is clear that the new Lagrangian would then generate the CSW (or MHV) rules of [1], and, once we have a Lagrangian we are much closer to being able to generalise the rules beyond tree-level. However, this cannot be correct as the rules cannot generate the one-loop amplitudes for processes in which the gluons all have positive helicity. These amplitudes have long been considered to be related to an anomaly [18]. In the context of the change of variables from \mathcal{A} to \mathcal{B} this anomaly could be related to the Jacobian which ought to be unity since the transformation is canonical. However, in [15] it was shown instead that these amplitudes result from an evasion of the equivalence theorem when the theory is formulated using dimensional regularisation. This implies a flaw in the argument we have just presented. Specifically, it was shown that in the case of the four-point all-plus amplitude the change of variables can be implemented with unit Jacobian by directly comparing both sides of:

$$\begin{aligned} \lim_{p_i^2 \rightarrow 0} \int \mathcal{D}(\mathcal{A}, \bar{\mathcal{A}}) e^{iS_{lc}} p_1^2 \bar{\mathcal{A}}^{a_1}(p_1) \dots p_4^2 \bar{\mathcal{A}}^{a_4}(p_4) = \\ \lim_{p_i^2 \rightarrow 0} \int \mathcal{D}(\mathcal{B}, \bar{\mathcal{B}}) e^{iS_{MHV}} p_1^2 \{\bar{\mathcal{B}}^{a_1}(p_1) + \dots\} \dots p_4^2 \{\bar{\mathcal{B}}^{a_4}(p_4) + \dots\} \end{aligned} \quad (1.13)$$

where the dots in $\bar{\mathcal{B}}(p_1) + \dots$ represent the extra terms involving the Ξ in (1.11). If we ignored these extra terms, as the S-matrix equivalence theorem implies we should, then the right-hand side would vanish because there are no interactions in S_{MHV} that would allow us to contract all the $\bar{\mathcal{B}}$ together. Since it is known that this amplitude is in fact non-zero the extra terms must contribute and the equivalence theorem is not directly applicable. These extra terms appear to spoil the efficiency of our approach. If we have to include the details of the transformation in computing scattering amplitudes then we are unlikely to be able to profit from any gains resulting from the simplicity of the MHV Lagrangian. It is the purpose of this paper to investigate just how damaging this is. We will see that actually the problem is quite contained and the equivalence theorem is only spoilt for a class of known amplitudes.

To simplify our discussion we will regulate using Four-Dimensional-Helicity regularisation [19] in which the external helicity are in four dimensions and only the internal momenta are in D dimensions. It is not essential to use this scheme, and in our earlier paper [15] we used standard dimensional regularisation, but it will simplify our expressions considerably. In section 2, we will describe this. Then in section 3, we examine the canonical transformation using it. We will find that the effect of regularisation is to make only minor changes to the recursion relations for the expansion coefficients. In order to avoid

spurious poles in the recursion expansion of Ξ^s , we also establish a new recursion relation of Ξ^s which involves only true singularities in each term of the expansion. As a byproduct we also find a relation between the tree-level light-cone diagrams and the canonical expansion coefficients, which will facilitate the singularity analysis in the translation kernel contribution later. We also review the tree-level evasion of the equivalence theorem for the $(-++)$ amplitude in section 4.

After this preparation, in section 5, we will discuss systematically the different ways that the S-matrix equivalence theorem can be evaded. We first argue that at tree-level evasion will not occur in higher point amplitudes. Then we discuss the three ways that the theorem can potentially be evaded at one-loop: by dressing propagators, in tadpoles, and by infrared divergences. We will conclude that only tadpoles can evade the equivalence theorem at one-loop. During this discussion, we find that there is a puzzle in the $(++-)$ amplitude with an external leg dressed by a tadpole. By examining the calculation of the $(+++)$ amplitude in section 6, we find that the one-minus-helicity amplitudes should come just from tadpoles made out of MHV vertices, but when we cut the diagrams there appear to be additional contributions from equivalence theorem evading tadpoles which can dress external legs. In section 7, we resolve this double-counting puzzle by choosing a suitable limiting order in the LSZ procedure and show that these extra terms do not contribute to the on-shell amplitude. Section 8 is the conclusion.

2. Dimensional Regularisation

We will regulate the ultra-violet divergences of pure Yang-Mills by working in arbitrary space-time dimension, D , and using co-ordinates which replace the pair z, \bar{z} of complex space-like co-ordinates by $D/2 - 1$ such pairs, $z_{(i)}, \bar{z}_{(i)}$. In [15] we used standard dimensional regularisation in which the gauge-field A_μ has D space-time components. We could instead use four-dimensional-helicity regularization (FDH) [19] and keep μ four dimensional. Consequently polarisation vectors would remain four dimensional, so we retain just two helicities, and the gauge invariance of the action is four dimensional. Just as in the usual dimensional regularisation the momenta of ‘physical’ gluons which appear in asymptotic states of scattering processes also remain in four dimensions, but the momenta of virtual gluons that appear as internal lines in Feynman diagrams will be D dimensional. The advantage of FDH is that the light-cone gauge action is very similar to the four dimensional version, the only change being in the free part which becomes

$$\mathcal{L}^{-+} = \text{tr} \bar{\mathcal{A}} \left(\check{\partial} \hat{\partial} - \sum_{i=1}^{D/2-1} \partial_{(i)} \bar{\partial}_{(i)} \right) \mathcal{A}.$$

Tree-level amplitudes are unchanged when the external legs all have four dimensional momenta, however when the external legs are allowed to have D dimensional momenta then they are modified. In particular the amplitudes in which all but one of the scattered gluons have the same helicity no longer vanish. This is responsible for the non-vanishing of the one-loop amplitude in which all the scattered gluons have the same helicity because

the optical theorem relates the imaginary part of this latter amplitude to the product of tree-level amplitudes of the former. The one-loop four-gluon all positive helicity reduced amplitude is [20]

$$-\frac{ig^4}{48\pi^2} \frac{\{p_1, p_2\} \{p_3, p_4\}}{(p_1, p_2)(p_3, p_4)} \quad (2.1)$$

where p_1, \dots, p_4 are the momenta of the gluons and $\{p_1, p_2\} \equiv \hat{p}_1 \bar{p}_2 - \hat{p}_2 \bar{p}_1$. The all-plus one-loop amplitudes are missing from a naïve application of the MHV rules at one-loop because if we are limited to vertices of Parke-Taylor type then we cannot construct such amplitudes. (In [15] it was shown that such amplitudes originate in a failure of the S-matrix equivalence of the \mathcal{A} and \mathcal{B} fields, we shall enlarge on this later.)

The failure of the one minus rest plus helicity tree-level amplitudes to vanish has significant consequences for the attempt to construct an MHV Lagrangian in D dimensions. Firstly it means that the theory described by the truncated Lagrangian $\mathcal{L}^{-+} + \mathcal{L}^{-++}$ that generates these amplitudes is not free. Secondly it means that the Parke-Taylor vertices are likely to be much more complicated in D dimensions because their simplicity in four dimensions can be explained within the BCFW recursion method [3] as deriving from the vanishing of the one minus rest plus tree-level amplitude. We will now investigate how damaging these facts are.

3. Canonical transformation in D dimensions

3.1 Recursion relations for the expansion coefficients

Perhaps surprisingly we can still construct a canonical transformation in D dimensions so that (1.7) holds. Using FDH regularization, and given (1.8) we have to solve

$$\omega \mathcal{A}(x) + \mathcal{A}(x) \left(\frac{\bar{\partial}}{\partial} \mathcal{A}(x) \right) - \left(\frac{\bar{\partial}}{\partial} \mathcal{A}(x) \right) \mathcal{A}(x) = \int_{\hat{x}=const.} \omega' \mathcal{B}(x') \frac{\delta \mathcal{A}(x)}{\delta \mathcal{B}(x')} d^{D-1} x' \quad (3.1)$$

where

$$\omega = \sum_{i=1}^{D/2-1} \partial_{(i)} \bar{\partial}_{(i)} / \partial.$$

Re-arranging:

$$\omega \mathcal{A}(x) - \int_{\hat{x}=const.} \omega' \mathcal{B}(x') \frac{\delta \mathcal{A}(x)}{\delta \mathcal{B}(x')} d^{D-1} x' = -\mathcal{A}(x) \left(\frac{\bar{\partial}}{\partial} \mathcal{A}(x) \right) + \left(\frac{\bar{\partial}}{\partial} \mathcal{A}(x) \right) \mathcal{A}(x). \quad (3.2)$$

We make the basic assumption, appropriate to perturbation theory, that we can expand the Fourier transform of \mathcal{A} in powers of the transform of \mathcal{B} , with kernels Υ . (Note we use the same symbol for the fields and their Fourier transforms)

$$\mathcal{A}_p = \sum_{n=1}^{\infty} \int \Upsilon(p, p_1, \dots, p_n) \delta(p + \sum_{i=1}^n p_i) \mathcal{B}_{\bar{1}} \dots \mathcal{B}_{\bar{n}} d^D p_1 \dots d^D p_n, \quad (3.3)$$

where we adopt the notation that the subscripts of the fields label the momenta: $\mathcal{A}_p \equiv \mathcal{A}(p)$ and $\mathcal{B}_{\bar{i}} \equiv \mathcal{B}(-p_i)$. Then the first term on the left-hand-side of (3.2) multiplies each term in

the expansion by the Fourier transform of ω , $i\Omega_0 \equiv i\Omega(p)$, whereas the second replaces each \mathcal{B}_i by $i\Omega_i\mathcal{B}_i$, and the right-hand-side glues two expansions together using what is essentially the three-point vertex corresponding to helicities $++-$ (and which we are attempting to eliminate from the theory by performing the canonical transformation to new variables). This is most easily represented graphically. Let us denote the expansion (3.3) by

$$\mathcal{A} = \text{---}\bullet\text{---}\textcircled{1}\text{---}\mathcal{B} + \text{---}\bullet\text{---}\textcircled{2}\begin{array}{l} \mathcal{B} \\ \mathcal{B} \end{array} + \text{---}\bullet\text{---}\textcircled{3}\begin{array}{l} \mathcal{B} \\ \mathcal{B} \\ \mathcal{B} \end{array} + \dots \quad (3.4)$$

and the Fourier transform of the right-hand-side of (3.2) by

$$\begin{array}{c} j \\ \diagup \\ i\text{---}\bullet\text{---}\bullet\text{---} \\ \diagdown \\ k \end{array} = \bar{V}^2(p_j, p_k, p_i)/\hat{p}_i,$$

where $\bar{V}^2(p_1, p_2, p_3) = i(\bar{1}/\hat{1} - \bar{2}/\hat{2})\hat{3}$ is the factor from the three-point $(++-)$ vertex of the lagrangian (1.12). The small black dots in the diagram denote the minus-helicity end of the propagators. Then the terms in (3.2) with n \mathcal{B} fields give

$$\left(\sum_0^n \Omega_i\right) \text{---}\bullet\text{---}\textcircled{n}\begin{array}{l} \mathcal{B} \\ \vdots \\ \mathcal{B} \end{array} = -\sum_{r+s=n} \text{---}\bullet\text{---}\begin{array}{c} \textcircled{r} \\ \vdots \\ \textcircled{s} \end{array}\begin{array}{l} \mathcal{B} \\ \vdots \\ \mathcal{B} \end{array}$$

If we were to use usual dimensional regularisation rather than FDH, we would have arrived at the same graphical equation, but with indices attached to the lines and $\bar{V}^2(p_j, p_k, p_i) = i(\{p_i, p_j\}_K \delta_{IJ}/\hat{p}_k + \{p_k, p_i\}_J \delta_{KI}/\hat{p}_j)$, in the notation of [15]. We can divide through by $\sum \Omega$ when it is non-zero and obtain the recursion relation for Υ in momentum space

$$\Upsilon(\bar{1} \cdots \bar{n}) = \frac{1}{\hat{1}(\Omega_1 + \cdots + \Omega_n)} \sum_{j=2}^{n-1} \bar{V}^2(P_{2j}, P_{j+1, n}, 1) \Upsilon(-, \bar{2}, \dots, \bar{j}) \Upsilon(-, \overline{j+1}, \dots, \bar{n}) \quad (3.5)$$

where we use the notation $P_{i,j} = p_i + p_{i+1} + \cdots + p_j$, for $j > i$, $P_{i,j} = p_i + p_{i+1} + \cdots + p_n + p_1 + \cdots + p_j$ for $j < i$, $\bar{n} = -p_n$ and the $-$ in the bracket of Υ denotes the minus of the sum of all the other momenta in Υ . This can be represented graphically

$$\text{---}\bullet\text{---}\textcircled{n}\begin{array}{l} \mathcal{B} \\ \vdots \\ \mathcal{B} \end{array} = \frac{1}{\sum_0^n \Omega_i} \sum_{r+s=n} \text{---}\bullet\text{---}\begin{array}{c} \textcircled{r} \\ \vdots \\ \textcircled{s} \end{array}\begin{array}{l} \mathcal{B} \\ \vdots \\ \mathcal{B} \end{array}$$

We will encounter situations when $\sum \Omega$ vanishes, and then we need a prescription for dealing with this singularity. We will address this in the appendices.

If we denote $-1/(\sum_0^n \Omega_i)$ by a closed broken curve cutting each line whose momentum appears in the sum, each order of the expansion of \mathcal{A} can be represented as

$$\begin{array}{c} \text{---} \bullet (n) \begin{array}{l} \nearrow \mathcal{B}_1 \\ \vdots \\ \searrow \mathcal{B}_n \end{array} = - \sum_{r+s=n} \text{---} \bullet \left(\begin{array}{c} \text{---} \bullet \begin{array}{l} \nearrow \mathcal{B}_1 \\ \vdots \\ \searrow \mathcal{B}_r \end{array} \\ \vdots \\ \text{---} \bullet \begin{array}{l} \nearrow \mathcal{B}_s \\ \vdots \\ \searrow \mathcal{B}_n \end{array} \end{array} \right. \end{array} \quad (3.6)$$

where

$$\bar{p} \text{---} \bullet (n) \begin{array}{l} \nearrow \mathcal{B}_1 \\ \vdots \\ \searrow \mathcal{B}_n \end{array} = \int_{1\dots n} \Upsilon(\bar{p}\bar{1} \dots \bar{n}) \mathcal{B}_1 \dots \mathcal{B}_n.$$

This can be easily iterated, starting with the leading term $\mathcal{A} = \mathcal{B}$:

$$\begin{aligned} \mathcal{A} = & \mathcal{B} - \text{---} \bullet \left(\begin{array}{c} \text{---} \bullet \mathcal{B} \\ \vdots \\ \text{---} \bullet \mathcal{B} \end{array} \right) + \text{---} \bullet \left(\begin{array}{c} \text{---} \bullet \left(\begin{array}{c} \text{---} \bullet \mathcal{B} \\ \vdots \\ \text{---} \bullet \mathcal{B} \end{array} \right) \\ \vdots \\ \text{---} \bullet \mathcal{B} \end{array} \right) \\ & + \text{---} \bullet \left(\begin{array}{c} \text{---} \bullet \left(\begin{array}{c} \text{---} \bullet \left(\begin{array}{c} \text{---} \bullet \mathcal{B} \\ \vdots \\ \text{---} \bullet \mathcal{B} \end{array} \right) \\ \vdots \\ \text{---} \bullet \mathcal{B} \end{array} \right) \\ \vdots \\ \text{---} \bullet \mathcal{B} \end{array} \right) + \dots \end{aligned}$$

Similarly we can expand $\bar{\mathcal{A}}$ in terms of \mathcal{B} , and $\bar{\mathcal{B}}$ in which it is linear. It is more convenient to expand $\hat{\partial}\bar{\mathcal{A}}$ in terms of \mathcal{B} , and $\hat{\partial}\bar{\mathcal{B}}$, and we denote this graphically by

$$\begin{aligned} \hat{\partial}\bar{\mathcal{A}} = & \text{---} \bullet \hat{\partial}\bar{\mathcal{B}} + \text{---} \bullet \left(\begin{array}{c} \hat{\partial}\bar{\mathcal{B}} \\ \vdots \\ \mathcal{B} \end{array} \right) + \text{---} \bullet \left(\begin{array}{c} \mathcal{B} \\ \vdots \\ \hat{\partial}\bar{\mathcal{B}} \end{array} \right) \\ & + \text{---} \bullet \left(\begin{array}{c} \mathcal{B} \\ \vdots \\ \hat{\partial}\bar{\mathcal{B}} \end{array} \right) + \text{---} \bullet \left(\begin{array}{c} \hat{\partial}\bar{\mathcal{B}} \\ \vdots \\ \mathcal{B} \end{array} \right) + \text{---} \bullet \left(\begin{array}{c} \mathcal{B} \\ \vdots \\ \hat{\partial}\bar{\mathcal{B}} \end{array} \right) + \dots \end{aligned}$$

and in momentum space we use Ξ to denote the expansion coefficients

$$\bar{p} \text{---} \bullet (n) \begin{array}{l} \nearrow \mathcal{B}_1 \\ \vdots \\ \searrow \mathcal{B}_n \end{array} = \int_{1\dots n} \hat{\imath} \Xi^i(\bar{p}\bar{1} \dots \bar{n}) \mathcal{B}_1 \dots \bar{\mathcal{B}}_i \dots \mathcal{B}_n.$$

Using this and (3.4) allows us to depict the second of (1.8) as

$$\hat{\partial}\bar{\mathcal{B}} = \Sigma \text{ [Diagram: A white circle with four external lines labeled } \mathcal{B} \text{ and a black dot on its right side, connected to a grey circle with four external lines labeled } \mathcal{B} \text{ and a black dot on its left side, which is connected to } \hat{\partial}\bar{\mathcal{B}} \text{]}.$$

Since there are no \mathcal{B} -fields on the left-hand-side we can equate to zero the sum of terms on the right that contain precisely n \mathcal{B} -fields, when $n > 0$:

$$0 = \Sigma \text{ [Diagram: A white circle with four external lines labeled } \mathcal{B} \text{ and a black dot on its right side, connected to a grey circle with four external lines labeled } \mathcal{B} \text{ and a black dot on its left side, which is connected to } \hat{\partial}\bar{\mathcal{B}} \text{]}.$$

The term in which there are no \mathcal{B} -fields in the left-hand factor is the kernel we are looking for, so

$$\text{[Diagram: A grey circle with four external lines labeled } \mathcal{B} \text{ and a black dot on its left side, which is connected to } \hat{\partial}\bar{\mathcal{B}} \text{]} = -\Sigma' \text{ [Diagram: A white circle with four external lines labeled } \mathcal{B} \text{ and a black dot on its right side, connected to a grey circle with four external lines labeled } \mathcal{B} \text{ and a black dot on its left side, which is connected to } \hat{\partial}\bar{\mathcal{B}} \text{]} \quad (3.7)$$

where the prime on the sum indicates that we sum over terms in which there is at least one \mathcal{B} -field in the left-hand factor, and the ordering of fields matches on both sides of the equation. This is iterated to yield

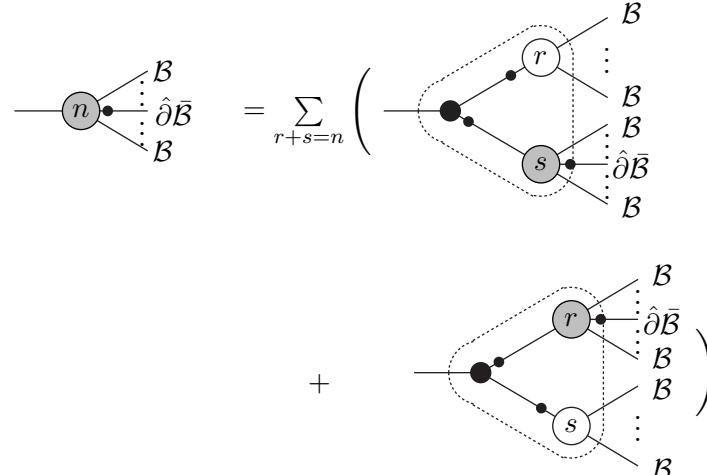
$$\begin{aligned} \hat{\partial}\bar{\mathcal{A}} = \hat{\partial}\bar{\mathcal{B}} &+ \text{[Diagram: A black dot with two external lines labeled } \mathcal{B} \text{ and } \hat{\partial}\bar{\mathcal{B}} \text{, enclosed in a dashed circle]} + \text{[Diagram: A black dot with two external lines labeled } \mathcal{B} \text{ and } \hat{\partial}\bar{\mathcal{B}} \text{, enclosed in a dashed circle]} - \text{[Diagram: A black dot with two external lines labeled } \mathcal{B} \text{ and } \hat{\partial}\bar{\mathcal{B}} \text{, enclosed in a dashed oval]} \\ &- \text{[Diagram: A black dot with two external lines labeled } \mathcal{B} \text{ and } \hat{\partial}\bar{\mathcal{B}} \text{, enclosed in a dashed oval]} + \text{[Diagram: A black dot with two external lines labeled } \mathcal{B} \text{ and } \hat{\partial}\bar{\mathcal{B}} \text{, enclosed in a dashed oval]} + \dots \end{aligned} \quad (3.8)$$

However, the broken curves in the above diagrams do not denote the real singularities in the expansion of $\bar{\mathcal{A}}$. Some singularities are cancelled out. For example, by explicit calculation, one finds that the singularity represented by the inner broken curves around the left big black dot in the fifth and sixth terms are cancelled out. In fact, by induction, one can

prove another recursion relation of Ξ^s :

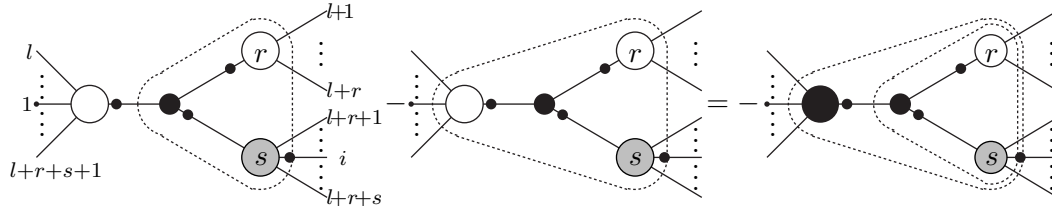
$$\begin{aligned} \Xi_{1,\dots,\bar{n}}^{i-1} = & -\frac{1}{\Omega_1 + \dots + \Omega_n} \left(\sum_{l=2}^{i-1} \frac{1}{\hat{P}_{l+1,n}} \bar{V}^2(p_1, P_{2,l}, P_{l+1,n}) \Upsilon(-, \bar{2}, \dots, \bar{l}) \Xi^{i-l}(-, \overline{l+1}, \dots, \bar{n}) \right. \\ & \left. + \sum_{l=i}^{n-1} \frac{1}{\hat{P}_{2,l}} \bar{V}^2(P_{l+1,n}, p_1, P_{2,l}) \Xi^{i-1}(-, \bar{2}, \dots, \bar{l}) \Upsilon(-, \overline{l+1}, \dots, \bar{n}) \right). \end{aligned} \quad (3.9)$$

Using this we can represent each order of the expansion of $\hat{\partial}\bar{\mathcal{A}}$ by diagrams:



$$= \sum_{r+s=n} \left(\text{Diagram 1} + \text{Diagram 2} \right) \quad (3.10)$$

The proof of the new recursion relation starts with the old one (3.7) and uses relation



$$= - \text{Diagram 3} \quad (3.11)$$

repeatedly (see appendix B for a sketch of the proof). The relation above is simply a result of the equation

$$\frac{1}{\Omega_{l+r+s+1,l} + \sum_{i=l+1}^{l+r+s} \Omega_i} - \frac{1}{\sum_{i=1}^n \Omega_i} = \frac{\Omega_{l+1,l+r+s} + \sum_{i=l+r+s+1}^l \Omega_i}{(\Omega_{l+r+s+1,l} + \sum_{i=1}^{l+1} \Omega_{l+r+s}) \sum_{i=1}^n \Omega_i} \quad (3.12)$$

where $\Omega_{i,j} = P_{i,j} \bar{P}_{i,j} / \hat{P}_{i,j}$. The numerator on the right-hand-side of (3.12) will cancel the denominator of the left Υ blob in the diagrams. We denote this cancellation by filling in the left-hand blob. In fact, there is an easy way to prove this recursion relation in four dimensions where we do not care about regularization: If we use the relation obtained in

[16]

$$\Xi^{i-1}(1 \cdots n) = -\frac{\hat{i}}{\hat{1}} \Upsilon(1 \cdots n), \quad (3.13)$$

this recursion relation recovers that of (3.6) for Υ .

3.2 Reconstructing the expansion coefficients from tree-level light-cone diagrams

From (3.5) we observe that the expansion terms of \mathcal{A} can be constructed as follows: for each term of the expansion, draw all the tree-level Feynman diagrams with an \mathcal{A} as one end of an external propagator and all \mathcal{B} s in the term as amputated external lines using only $(++-)$ vertices; then calculate this diagram using \bar{V}^2 as vertices and $1/(\hat{p}(\Omega_p + \sum \Omega))$ as corresponding propagators. Notice that the light-cone Feynman rule for vertex $(++-)$ is

$$\bar{V}(1, 2, 3) = i \frac{4}{g^2} \bar{V}^2(\bar{1}, \bar{2}, \bar{3}) = -i \frac{4}{g^2} \bar{V}^2(1, 2, 3) \quad (3.14)$$

and the light-cone propagator is

$$\langle \mathcal{A}_p \mathcal{A}_{\bar{p}} \rangle = -i \frac{g^2}{2p^2}. \quad (3.15)$$

So

$$\langle \mathcal{A}_3 \mathcal{A}_{\bar{3}} \rangle \bar{V}(1, 2, 3) = -\frac{2}{p_3^2} \bar{V}^2(1, 2, 3) \quad (3.16)$$

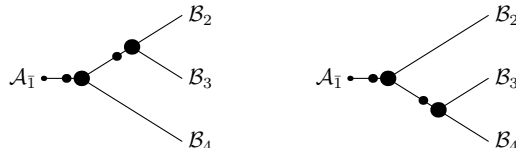
is consistent with the coefficient of each term in the recursion relation if we make the replacement $-2/p_3^2 \rightarrow 1/(\hat{p}_3(\Omega_3 + \Omega_1 + \Omega_2))$. As a result, we can reconstruct the terms of \mathcal{A} from light-cone tree-level calculations by replacing the light-cone propagators using

$$\frac{1}{P_{ij}^2} \rightarrow -\frac{1}{2\hat{P}_{j+1,i-1}(\Omega_{j+1,i-1} + \Omega_i + \Omega_{i+1} + \cdots + \Omega_j)}. \quad (3.17)$$

Here $P_{j+1,i-1}$ should be understood as the sum of all momenta except those labelled from i to j . The momentum in each term in the bracket of the denominators corresponds to the outgoing momentum of the external line of the sub-tree diagram not involving \mathcal{A} when the propagator is cut. For example, for terms with $\mathcal{B}_2 \mathcal{B}_3 \mathcal{B}_4$:

$$\begin{aligned} \mathcal{A}_{\bar{1}} &\sim \Upsilon(\bar{1}\bar{2}\bar{3}\bar{4}) \mathcal{B}_2 \mathcal{B}_3 \mathcal{B}_4 \\ &= \frac{1}{\hat{1}(\Omega_1 + \cdots + \Omega_4)} \left(\frac{\bar{V}^2(2, 34, 1) \bar{V}^2(3, 4, 12)}{\hat{P}_{12}(\Omega_{12} + \Omega_3 + \Omega_4)} + \frac{\bar{V}^2(23, 4, 1) \bar{V}^2(2, 3, 41)}{\hat{P}_{41}(\Omega_{41} + \Omega_2 + \Omega_3)} \right) \\ &\quad \times \mathcal{B}_2 \mathcal{B}_3 \mathcal{B}_4. \end{aligned} \quad (3.18)$$

The corresponding diagrams are:



From the light-cone calculation of these Feynman diagrams, we have:

$$2^2 \frac{1}{p_1^2} \left(\frac{\bar{V}^2(2, 34, 1) \bar{V}^2(3, 4, 12)}{P_{12}^2} + \frac{\bar{V}^2(23, 4, 1) \bar{V}^2(2, 3, 41)}{P_{41}^2} \right) \quad (3.19)$$

in which the two terms correspond to the two tree-level Feynman diagrams. We can see that (3.18) and (3.19) only differ by the change

$$1/p_1^2 \rightarrow -1/(2\hat{1}(\Omega_1 + \cdots + \Omega_4)), \quad (3.20)$$

$$1/P_{12}^2 \rightarrow -1/(2\hat{P}_{12}(\Omega_{12} + \Omega_3 + \Omega_4)), \quad (3.21)$$

$$1/P_{41}^2 \rightarrow -1/(2\hat{P}_{41}(\Omega_{41} + \Omega_2 + \Omega_3)). \quad (3.22)$$

If we put p_2, p_3, p_4 on shell, the \rightarrow in the above equations can be replaced by $=$, thus (3.18) is equal to (3.19) which gives the translation kernel contribution to the amplitude as it should.

For $\bar{\mathcal{A}}$, the same rule also holds allowing us to reconstruct the expansion of $\bar{\mathcal{A}}$ from light-cone calculations: one needs to first draw the tree-level diagrams with one $\bar{\mathcal{A}}$ as an external propagator, all the $\mathcal{B}, \bar{\mathcal{B}}$ in the term as amputated legs using $(++-)$ vertices, and then calculate the diagram using the light-cone Feynman rules with the replacement (3.17). This can be justified from the recursion relation (3.9) with a similar discussion to that for Υ : First, in (3.9) all the Υ 's already obey this rule. The $-1/\hat{P}_{l+1,n} = 1/\hat{P}_{1,l}$ in the first term in the bracket will combine with the $1/\sum \Omega$ factor in the expansion of the next Ξ in this term to be $1/(P_{1,l}(\Omega_{1,l} + \sum_{i=l+1}^n \Omega_i))$ which is just what we need to be consistent with the rule. It is the same for the second term in the bracket. We only need to consider the factor of the Ξ in the first iteration and the last iteration. We should divide the expansion of $\hat{\partial}\bar{\mathcal{A}}$ by the corresponding $i\hat{p}$ in the momentum space, to obtain the expansion of $\bar{\mathcal{A}}$. This factor $1/\hat{p}_1$ will combine with the factor of the first Ξ to be $1/(\hat{p}_1(\sum_{i=1}^n \Omega_i))$ in (3.9). The last iteration corresponds to the right-most grey blob adjacent to $\hat{\partial}\mathcal{B}$ in each term of the full iteratively expanded diagrams in (3.10). The extra factor $1/\hat{i}$ in the Ξ of the last step of the iteration will cancel the \hat{i} in the $i\mathcal{B}_i$ from $\hat{\partial}\mathcal{B}$. So just as in the case of Υ , the expansion of $\bar{\mathcal{A}}$ requires calculating tree-level diagrams using \bar{V}^2 as vertices and $1/(\hat{p}(\Omega_p + \sum \Omega))$ as the propagators, and so obeys the same rule.

4. ‘Missing’ amplitudes from equivalence theorem evasion reviewed

In [15] we explained how the tree-level $(-++)$ and the one-loop $(++\cdots++)$ amplitudes are obtained from the $\mathcal{B}, \bar{\mathcal{B}}$ theory, despite there being no vertices in this theory that could contribute. The amplitudes are non-zero because the equivalence theorem is not directly applicable to our non-local transformation. Thus \mathcal{A} and $\bar{\mathcal{A}}$ do not create the same particles as $\mathcal{B}, \bar{\mathcal{B}}$. This would appear to drastically complicate the calculation of amplitudes within the $\mathcal{B}, \bar{\mathcal{B}}$ theory. It is the main purpose of this paper to show that only certain amplitudes are affected by this, and that in the general case we can use either set of fields to generate amplitudes. In this section we briefly review the ‘missing’ tree-level amplitude.

In light-cone gauge Yang-Mills theory the tree-level contribution to the Green function $\langle \mathcal{A}(p_1) \bar{\mathcal{A}}(p_2) \bar{\mathcal{A}}(p_3) \rangle$ comes from the vertex in \mathcal{L}^{-++} , so to this order, and taking account

of the $i\epsilon$ -prescription in propagators (and suppressing Lie algebra indices on the understanding that we deal with colour-ordered amplitudes)

$$(p_1^2 + i\epsilon)(p_2^2 + i\epsilon)(p_3^2 + i\epsilon) \langle \mathcal{A}(p_1) \bar{\mathcal{A}}(p_2) \bar{\mathcal{A}}(p_3) \rangle = \left(p_1 \text{---} \bullet \begin{array}{l} \nearrow p_2 \\ \searrow p_3 \end{array} \right) \hat{p}_1,$$

and as all three momenta go on-shell this becomes the three-point amplitude (which vanishes in four dimensional Minkowski space, but is non-zero in other signatures and dimensions.) Clearly $\langle \mathcal{B}(p_1) \bar{\mathcal{B}}(p_2) \bar{\mathcal{B}}(p_3) \rangle = 0$ at tree-level due to the helicity assignment of the Parke-Taylor vertices. To compute the Green function in the $\mathcal{B}, \bar{\mathcal{B}}$ theory we must use the translation kernels:

$$\begin{aligned} \langle \mathcal{A}(p_1) \bar{\mathcal{A}}(p_2) \bar{\mathcal{A}}(p_3) \rangle &= -\langle \left(\mathcal{B}(p_1) + p_1 \text{---} \bullet \begin{array}{l} \nearrow \mathcal{B} \\ \searrow \mathcal{B} \end{array} + \dots \right) \times \\ &\quad \frac{1}{\hat{p}_2} \left(\hat{\partial} \bar{\mathcal{B}}(p_2) - p_2 \text{---} \bullet \begin{array}{l} \nearrow \mathcal{B} \\ \searrow \hat{\partial} \bar{\mathcal{B}} \end{array} - p_2 \text{---} \bullet \begin{array}{l} \nearrow \hat{\partial} \bar{\mathcal{B}} \\ \searrow \mathcal{B} \end{array} + \dots \right) \times \\ &\quad \frac{1}{\hat{p}_3} \left(\hat{\partial} \bar{\mathcal{B}}(p_3) - p_3 \text{---} \bullet \begin{array}{l} \nearrow \mathcal{B} \\ \searrow \hat{\partial} \bar{\mathcal{B}} \end{array} - p_3 \text{---} \bullet \begin{array}{l} \nearrow \hat{\partial} \bar{\mathcal{B}} \\ \searrow \mathcal{B} \end{array} + \dots \right) \rangle \end{aligned}$$

since no vertices contribute to leading order this can be computed by contracting the $\mathcal{B}, \bar{\mathcal{B}}$ fields using the free propagator, which we denote by \sim

$$\begin{aligned} \langle \mathcal{A}(p_1) \bar{\mathcal{A}}(p_2) \bar{\mathcal{A}}(p_3) \rangle &= \\ &= \left(p_1 \text{---} \bullet \begin{array}{l} \nearrow p_2 \\ \searrow p_3 \end{array} \right) + \left(p_1 \text{---} \bullet \begin{array}{l} \nearrow p_2 \\ \searrow p_3 \end{array} \right) \frac{\hat{p}_1}{\hat{p}_2} + \left(p_1 \text{---} \bullet \begin{array}{l} \nearrow p_2 \\ \searrow p_3 \end{array} \right) \frac{\hat{p}_1}{\hat{p}_3} \\ &= \left(p_1 \text{---} \bullet \begin{array}{l} \nearrow p_2 \\ \searrow p_3 \end{array} \right) \frac{\hat{p}_1}{(p_1^2 + i\epsilon)(p_2^2 + i\epsilon)(p_3^2 + i\epsilon)} \left(\frac{p_1^2 + i\epsilon}{\hat{p}_1} + \frac{p_2^2 + i\epsilon}{\hat{p}_2} + \frac{p_3^2 + i\epsilon}{\hat{p}_3} \right), \end{aligned}$$

The broken line cutting the three lines denotes division by

$$-\sum_j \Omega(p_j) = -\sum_j \sum_{i=1}^{D/2-1} p_{j(i)} \bar{p}_{j(i)} / \hat{p}_j,$$

which does not depend on the \check{p}_j . However, if we add $\sum_j \check{p}_j$, which vanishes by momentum conservation, this becomes $\sum_j p_j^2 / \hat{p}_j$. If we also include $i\epsilon$ terms to match the last factor then we reproduce the light-cone Yang-Mills amplitude. This tells us how to treat $1/\sum \Omega$

when the denominator is singular, so in general the broken lines in our diagrams will denote

$$\frac{1}{\sum_j \frac{p_j^2 + i\epsilon}{\hat{p}_j}}.$$

It is of course not surprising that we reproduce the usual Green function, as all we have done is transform to new variables to do the calculation. It will be useful, for what comes later, to examine how the equivalence theorem has been evaded. Note that the combined limit $p_1^2 + i\epsilon, p_2^2 + i\epsilon, p_3^2 + i\epsilon \rightarrow 0$ is not valid for each term separately, because the value of

$$\lim_{p_1 + i\epsilon^2, p_2^2 + i\epsilon, p_3^2 + i\epsilon \rightarrow 0} \frac{p_1^2 + i\epsilon}{\frac{p_1^2 + i\epsilon}{1} + \frac{p_2^2 + i\epsilon}{2} + \frac{p_3^2 + i\epsilon}{3}}$$

depends on the order in which the limits are taken, but it is valid to take the limit of the sum of the three terms because the factor $(p_1^2 + i\epsilon)/\hat{1} + (p_2^2 + i\epsilon)/\hat{2} + (p_3^2 + i\epsilon)/\hat{3}$ in the denominator is cancelled out. Consequently we can take the limit of the sum in any order. Suppose we take the legs on-shell one after another, beginning with p_2 and p_3 . We include ϵ in the mass-shell condition because it enters the propagators for external legs that have to be cancelled by the LSZ factors. Since $p_2^2 + i\epsilon$ and $p_3^2 + i\epsilon$ cancel the propagators in the first diagram, but not in the other two, it is clear that for general p_1 the contributions from the last two diagrams are wiped out in the limit leaving

$$\begin{aligned} \lim_{p_2^2 + i\epsilon \rightarrow 0} \lim_{p_3^2 + i\epsilon \rightarrow 0} (p_2^2 + i\epsilon) (p_3^2 + i\epsilon) \langle \mathcal{A}(p_1) \bar{\mathcal{A}}(p_2) \bar{\mathcal{A}}(p_3) \rangle = \\ \lim_{p_2^2 + i\epsilon \rightarrow 0} \lim_{p_3^2 + i\epsilon \rightarrow 0} (p_2^2 + i\epsilon) (p_3^2 + i\epsilon) \left(\text{Diagram 1} \right) = \\ \lim_{p_2^2 + i\epsilon \rightarrow 0} \lim_{p_3^2 + i\epsilon \rightarrow 0} \frac{1}{\frac{p_1^2 + i\epsilon}{\hat{p}_1} + \frac{p_2^2 + i\epsilon}{\hat{p}_2} + \frac{p_3^2 + i\epsilon}{\hat{p}_3}} \left(\text{Diagram 2} \right) = \\ \frac{\hat{p}_1}{p_1^2 + i\epsilon} \left(\text{Diagram 3} \right). \end{aligned}$$

So the $1/(p_1^2 + i\epsilon)$ needed to cancel the $p_1^2 + i\epsilon$ coming from the LSZ prescription is generated as part of the translation kernels, even though these appeared to be independent of the \tilde{p} components of momenta. We should point out that ‘missing amplitudes’ can be generated in different ways if the theory is formulated differently such as in the gauge fixing of the twistor action [22] or in the light-cone friendly regularisation of [23].

5. Equivalence theorem evasion in general.

When the equivalence theorem holds we can ignore all except the leading translation kernels. However the theorem will be evaded whenever the translation kernels that express

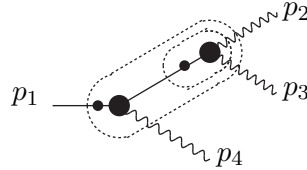
$\mathcal{A}(p)$ or $\bar{\mathcal{A}}(p)$ in terms of \mathcal{B} and $\bar{\mathcal{B}}$ produce a $1/(p^2 + i\epsilon)$ that can cancel the LSZ factors. We will now list all the types of process in which this can occur. The singular terms originate in the $1/\sum \Omega$ represented by the broken lines in our diagrams. These must cut the line with momentum p if we are to end up with $1/(p^2 + i\epsilon)$. Suppose that the other lines cut carry momenta p_1, \dots, p_n , then

$$\frac{1}{\sum \Omega} = \frac{1}{\frac{p^2 + i\epsilon}{\hat{p}} + \sum_{j=1}^n \frac{p_j^2 + i\epsilon}{\hat{p}_j}},$$

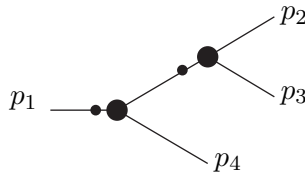
so we have to examine the conditions under which $\sum_{j=1}^n (p_j^2 + i\epsilon)/\hat{p}_j = 0$. Notice that here we actually take $\sum_{j=1}^n (p_j^2 + i\epsilon)/\hat{p}_j \rightarrow 0$ limit first and then $p^2 \rightarrow 0$ in the LSZ procedure. We will see that this is valid in a similar way to the three point case.

5.1 Tree-level

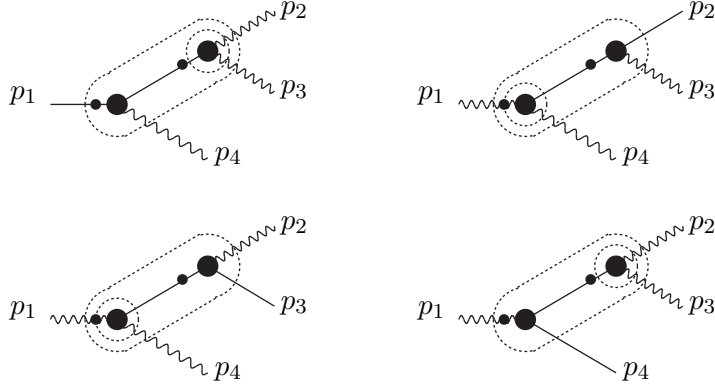
In the absence of loops there are two ways that $\sum_{j=1}^n (p_j^2 + i\epsilon)/\hat{p}_j = 0$. The first is that each of the legs cut by the broken line are external and so their momenta must be put on shell. For example, in the four-particle process with one $-$ helicity and three $+$ helicity gluons we need the Green function $\langle \mathcal{A}(p_1) \bar{\mathcal{A}}(p_2) \bar{\mathcal{A}}(p_3) \bar{\mathcal{A}}(p_4) \rangle$. Contributing to this are translation kernels for $\mathcal{A}(p_1)$, $\bar{\mathcal{A}}(p_2)$, $\bar{\mathcal{A}}(p_3)$, and $\bar{\mathcal{A}}(p_4)$ which give rise to diagrams like



in which four external legs are cut by the broken line. Since all the external lines will be cut by the broken curve we cannot include any Parke-Taylor vertices. Consequently, in the general case we can only ever have a contribution to a tree-level amplitude with one $-$ helicity external gluon and $n +$ helicity external gluons. For each light-cone tree-level diagram of such an amplitude, there are terms from the translation kernels that contribute. For example, for the four-point diagram:



using the method in section (3.2), we can construct the translation kernel contribution to this diagram from the canonical expansion of \mathcal{A}_1 , $\bar{\mathcal{A}}_2$, $\bar{\mathcal{A}}_3$, $\bar{\mathcal{A}}_4$ which can be represented graphically:



The difference between these translation kernels and the light-cone contribution is only in the denominators. Examining these:

$$\begin{aligned}
& \lim_{p_1^2, p_2^2, p_3^2, p_4^2 \rightarrow 0} p_1^2 p_2^2 p_3^2 p_4^2 \left\{ \frac{1}{\hat{1} \left(\frac{p_1^2}{1} + \frac{p_2^2}{2} + \frac{p_3^2}{3} + \frac{p_4^2}{4} \right) (\hat{1} + \hat{4}) \left(\frac{p_{41}^2}{1+4} + \frac{p_2^2}{2} + \frac{p_3^2}{3} \right) p_2^2 p_3^2 p_4^2} \right. \\
& + \frac{1}{\hat{2} \left(\frac{p_1^2}{1} + \frac{p_2^2}{2} + \frac{p_3^2}{3} + \frac{p_4^2}{4} \right) (\hat{2} + \hat{3}) \left(\frac{p_{23}^2}{2+3} + \frac{p_1^2}{1} + \frac{p_4^2}{4} \right) p_1^2 p_3^2 p_4^2} \\
& + \frac{1}{\hat{3} \left(\frac{p_1^2}{1} + \frac{p_2^2}{2} + \frac{p_3^2}{3} + \frac{p_4^2}{4} \right) (\hat{2} + \hat{3}) \left(\frac{p_{23}^2}{2+3} + \frac{p_1^2}{1} + \frac{p_4^2}{4} \right) p_1^2 p_2^2 p_4^2} \\
& \left. + \frac{1}{\hat{4} \left(\frac{p_1^2}{1} + \frac{p_2^2}{2} + \frac{p_3^2}{3} + \frac{p_4^2}{4} \right) (\hat{1} + \hat{4}) \left(\frac{p_{41}^2}{1+4} + \frac{p_2^2}{2} + \frac{p_3^2}{3} \right) p_1^2 p_2^2 p_3^2} \right\} \\
& = \lim_{p_1^2, p_2^2, p_3^2, p_4^2 \rightarrow 0} \frac{-\frac{p_{41}^2}{1+4} + \frac{p_1^2}{1} + \frac{p_4^2}{4} - \frac{p_2^2}{2} - \frac{p_3^2}{3}}{(\hat{1} + \hat{4}) \left(\frac{p_{41}^2}{1+4} + \frac{p_2^2}{2} + \frac{p_3^2}{3} \right) \left(-\frac{p_{41}^2}{1+4} + \frac{p_1^2}{1} + \frac{p_4^2}{4} \right)} \\
& = \frac{1}{p_{41}^2}, \tag{5.1}
\end{aligned}$$

(We omit the $+i\epsilon$ accompanying each p^2 here since it is not important in our discussion.) we see that the factor $p_1^2/\hat{1} + p_2^2/\hat{2} + p_3^2/\hat{3} + p_4^2/\hat{4}$ in the denominator is cancelled out and the limit procedure is valid at last. The denominator provides the propagator needed in the light-cone computation. Since the combined limit is valid, like in the $(++-)$ case, we could take the limit in any order, for example take the $p_1^2, p_2^2, p_3^2 \rightarrow 0$ first and then $p_4^2 \rightarrow 0$ at last. Then one finds the first three diagrams vanish and the contribution comes only from last diagram and the factor $\hat{4}(p_1^2/\hat{1} + p_2^2/\hat{2} + p_3^2/\hat{3} + p_4^2/\hat{4})$ becomes p_4^2 to be cancelled with p_4^2 in the numerator from the LSZ procedure. This reproduces the light-cone computation of the amplitude. One can imagine that the same thing happens for general multileg one-minus-helicity amplitudes. Fortunately these amplitudes vanish at tree-level in four dimensional Minkowski space, (and for $n > 2$ in arbitrary signature) which means that the translation kernel contributions add up to zero.

The other way that $\sum_{j=1}^n (p_j^2 + i\epsilon)/\hat{p}_j = 0$ without all of the p_j being external legs

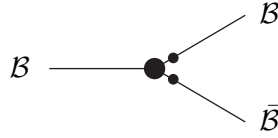
is if some of the terms in the sum cancel against each other, or if the translation kernel is connected to a vertex by a momentum that is on-shell. At tree-level this can only occur for special choices of the momenta of the external particles, and cannot contribute to an amplitude with generic values of external momenta. So at tree-level the equivalence theorem can be used for non-trivial generic amplitudes, which is why the MHV rules correctly reproduce tree-level amplitudes without having to take account of the translation between \mathcal{A} , $\bar{\mathcal{A}}$ and \mathcal{B} , $\bar{\mathcal{B}}$ fields.

5.2 One loop

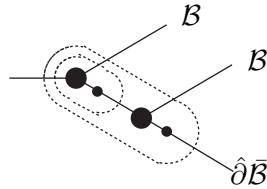
There are several processes that can occur at one-loop order that give rise to evasions of S-matrix equivalence. The first is that loops can dress the propagators that occur in tree-level diagrams. Secondly, we can have tadpole diagrams in which two legs of a translation kernel are contracted with each other. These diagrams are responsible for the all positive helicity amplitudes ‘missing’ from a straightforward application of the MHV rules. Thirdly we can have more general processes in which the loop integration has an infra-red divergence that might cancel the LSZ factor.

5.2.1 Dressing propagators

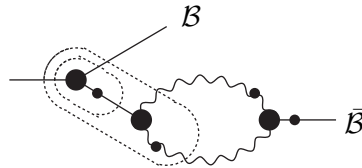
Loops can dress propagators, so, at one-loop, as for tree-level $\sum_{j=1}^n (p_j^2 + i\epsilon)/\hat{p}_j$ can vanish when each of the p_j is the momentum of an on-shell gluon. For example, the first interaction in (1.12), \mathcal{L}^{--+} which we denote by



can be contracted with the fifth term in the expansion of $\hat{\partial}\bar{\mathcal{A}}$ equation (3.8)

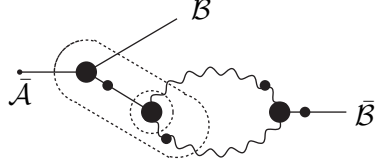


to give

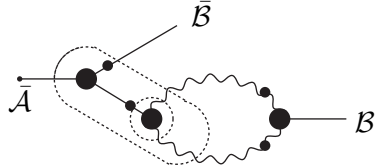


This will contribute to the Green function $\langle \mathcal{A}(p_1) \bar{\mathcal{A}}(p_2) \bar{\mathcal{A}}(p_3) \rangle$, for example by contracting \mathcal{B} with the leading term in the expansion of $\bar{\mathcal{A}}(p_2)$ and $\bar{\mathcal{B}}$ with that of $\mathcal{A}(p_1)$. The propagators cancel two of the LSZ factors for the $++-$ amplitude. Taking $p_2^2 + i\epsilon = 0$ and $p_1^2 + i\epsilon = 0$ causes the $1/\sum \Omega$ factor denoted by the inner broken curve to reduce

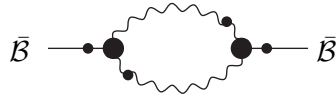
to $1/(p_3^2 + i\epsilon)$, which will cancel the remaining LSZ factor, thus evading the equivalence theorem and producing a contribution to the three-point amplitude that is the same as the tree-level diagram with a self-energy insertion on the p_1 leg. In Minkowski space the three-point amplitude vanishes on-shell anyway, so this evasion appears inconsequential. For complex on-shell momenta, of the kind used in the BCFW rules, this amplitude does not vanish, so it is worthwhile considering this further. We noted earlier that the relations (3.9) enable us to re-write the series for $\bar{\mathcal{A}}$ in a way that moves the position of the dotted lines so that the singularity $1/\sum_i \Omega_i$ corresponding to the dotted lines around the left big black dot is cancelled out after we sum the fifth and sixth term in (3.8). These combine to give



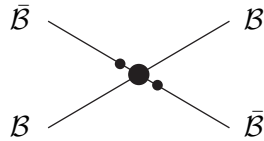
Since the contribution of the internal line to the denominator $\sum p_i^2/\hat{p}_i$ represented by the inner broken curve can not be zero, it is obvious that there is no $1/p^2$ generated in this diagram. So this diagram can not contribute to the amplitude. The same is true for the case of a dressed propagator on a \mathcal{B} leg:



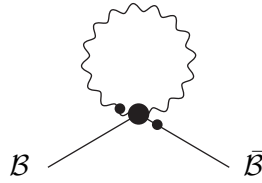
The three-point interaction can dress a propagator either in the way just described, or, potentially by two such vertices being glued together



An insertion of this kind into a diagram effectively changes a \mathcal{B} -field into a $\bar{\mathcal{B}}$ -field, however explicit calculation shows that this vanishes. At one-loop the only other vertices that can contribute to dressing propagators are contained in \mathcal{L}^{--++} :



and these produce insertions that connect \mathcal{B} with $\bar{\mathcal{B}}$

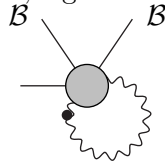


Dressing propagators can produce diagrams that evade the equivalence theorem, but only if the corresponding tree-level diagrams do so already, in which case the result is proportional to the tree-level amplitude. As we have seen this only happens for amplitudes that vanish in the physical dimension, so this source of equivalence theorem evasion has no physical consequence. However there is a subtlety involved in the one-loop $(++-)$ amplitude in $(++--)$ signature. In section 6, we will find that the tadpoles formed from MHV vertices already include the diagrams with external leg corrections. Including translation kernel contributions in the amplitude would appear to count the diagrams with external leg corrections twice. We will solve this puzzle in section 7.

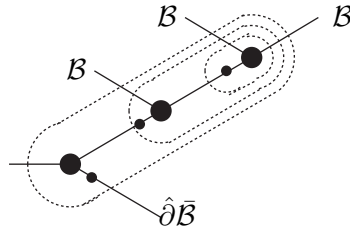
5.2.2 Tadpoles

At tree-level we dismissed the second way that $\sum_{j=1}^n (p_j^2 + i\epsilon)/\hat{p}_j$ could vanish because it could only apply to special configurations of external momenta. When we integrate over loop momenta such special configurations can easily arise, and so we must analyse them.

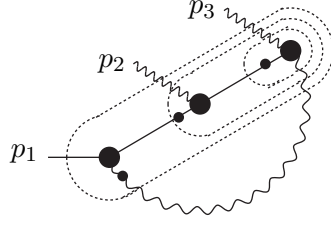
The simplest way that two of the terms in $\sum_{j=1}^n (p_j^2 + i\epsilon)/\hat{p}_j$ could cancel without each being on-shell occurs in the translation kernel for $\bar{\mathcal{A}}$ when a \mathcal{B} and $\bar{\mathcal{B}}$ field are contracted, because then their lines carry equal and opposite momenta. These are ‘tadpoles’ when drawn in terms of the translation kernels, e.g.



but are rather more complicated when drawn in terms of the graphical solution. For example, one of the terms contributing to this tadpole originates in the following term which appears in the expansion of $\bar{\mathcal{A}}$:



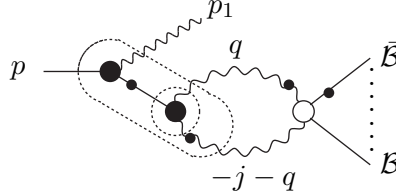
Contracting $\bar{\mathcal{B}}$ with a \mathcal{B} and the remaining fields with external gluons gives



When the p_2 and p_3 are put on-shell, $p_2^2 + i\epsilon = 0$ and $p_3^2 + i\epsilon = 0$, so the dotted line cutting the three external momenta and the gluon propagator reduces to $\sum_{j=1}^n (p_j^2 + i\epsilon)/\hat{p}_j = (p_1^2 + i\epsilon)/\hat{p}_1$ resulting in an evasion of S-matrix equivalence. Because the contraction used to make a tadpole removes a \mathcal{B} and a $\bar{\mathcal{B}}$ field from the translation kernels for $\bar{\mathcal{A}}$ they can contribute to one-loop amplitudes involving only positive helicity gluons. In [15] it was found that it is this mechanism that is responsible for generating the one-loop all plus four-point amplitude (2.1) that a naïve application of the MHV rules cannot account for.

5.2.3 Infra-red divergent loop integration

Evasion of S-matrix equivalence might arise in a more general situation when a vertex is attached to a translation kernel. For illustration we focus on one term in the expansion of $\bar{\mathcal{A}}$ and contract two of the legs with those of some arbitrary subgraph denoted by the open circle:



If we take $p_1^2 + i\epsilon = 0$, (having cancelled the corresponding LSZ factor with the propagator,) the loop integration is

$$\int d^D q \frac{1}{\frac{p^2+i\epsilon}{\hat{p}} + \frac{q^2+i\epsilon}{\hat{q}} - \frac{(q+j)^2+i\epsilon}{\hat{q}+\hat{j}}} \frac{1}{\frac{j^2+i\epsilon}{\hat{j}} + \frac{q^2+i\epsilon}{\hat{q}} - \frac{(q+j)^2+i\epsilon}{\hat{q}+\hat{j}}} \frac{1}{q^2 + i\epsilon} \frac{1}{(j+q)^2 + i\epsilon} f(j, q) \quad (5.2)$$

with $j = p + p_1$.

We need to investigate whether this integral can generate a factor of $1/(p^2 + i\epsilon)$. To do so it would have to be divergent as p goes on-shell. The integrand has a number of singularities as a function of the components of loop momentum q^μ but by deforming the integration contours into the complex q^μ -planes the surfaces where the integrand diverges can typically be avoided so that the integral is well-defined. We are aided in identifying the directions in which to deform the contours by the $i\epsilon$ prescription. (We can ignore what happens as $q \rightarrow \infty$ as the ultra-violet behaviour is regulated). However, as we vary p the positions of these singularities move, and it is possible that our integration surface may lie between several singularity surfaces that approach each other for some values of p and pinch the contours so that they can no longer be deformed to avoid the singularity. As this happens the value of the integral itself diverges as a function of p . Prior to taking the on-shell limit we can deform the integration surface so that it consists of a piece surrounding

the singularities and a piece that we can move well away from either singularity. In the on-shell limit we can ignore this last piece because of the LSZ factor, $p^2 + i\epsilon$. We now focus on the contribution from the piece surrounding the singularity, which means that in the loop integral we take $f(j, q)$ as constant. We begin by integrating out the \tilde{q} component. The first two factors of the integrand come from the translation kernels and so do not depend on \tilde{q} . As we close the \tilde{q} contour in the complex plane we pick up singularities from the propagators. Using conservation of momentum the residue can be put into a form similar to that of the kernel, but without $(p^2 + i\epsilon)/\hat{p}$:

$$\frac{\theta(\hat{q})\theta(-\hat{q} - \hat{j}) - \theta(-\hat{q})\theta(\hat{q} + \hat{j})}{\hat{q}(\hat{q} + \hat{j})} \frac{2\pi i}{\frac{q^2 + i\epsilon}{\hat{q}} - \frac{(q+j)^2 + i\epsilon}{\hat{q} + \hat{j}}} \quad (5.3)$$

which, of course, does not depend on \tilde{q} . This allows us to extract $1/(p^2 + i\epsilon)$ explicitly from the integral (5.2) which becomes

$$-\frac{2\pi i \hat{p}}{p^2 + i\epsilon} \int \left(\prod_{i=1}^{D/2-1} dq_{(i)} d\bar{q}_{(i)} \right) d\hat{q} \frac{\theta(\hat{q})\theta(-\hat{q} - \hat{j}) - \theta(-\hat{q})\theta(\hat{q} + \hat{j})}{\hat{q}(\hat{q} + \hat{j})} \quad (5.4)$$

$$\times \left[\frac{1}{\frac{p^2 + i\epsilon}{\hat{p}} + \frac{q^2 + i\epsilon}{\hat{q}} - \frac{(q+j)^2 + i\epsilon}{\hat{q} + \hat{j}}} - \frac{1}{\frac{q^2 + i\epsilon}{\hat{q}} - \frac{(q+j)^2 + i\epsilon}{\hat{q} + \hat{j}}} \right] f_1(j, q). \quad (5.5)$$

Since the second factor in the integrand of (5.2) is finite when the first factor is singular, it is irrelevant to our discussion and we absorb it into f_1 .

The LSZ factor is cancelled by the $1/(p^2 + i\epsilon)$. If we now take the on-shell limit $p^2 + i\epsilon \rightarrow 0$ then the two terms in square brackets cancel and the integral actually vanishes, provided that no singularity is encountered as we integrate over \hat{q} . However, for certain values of j and $q_{(i)}$ both terms in the square brackets are divergent close to the real axis, so we have to investigate the location of these singularities. The first diverges for

$$\hat{q} = \frac{-b \pm \sqrt{b^2 - 4a(c + i\epsilon\hat{j})}}{2a} \quad (5.6)$$

with

$$a = \phi - 2\hat{j}, \quad \phi = \frac{p^2 + i\epsilon}{\hat{p}}, \quad b = \hat{j}\phi - j^2 + 2 \sum_i (q_{(i)} \bar{j}_{(i)} + \bar{q}_{(i)} j_{(i)}), \quad c = -2\hat{j} \sum_i q_{(i)} \bar{q}_{(i)}, \quad (5.7)$$

whilst the location of the pole in the second term is given by the above expression with ϕ set to zero. For the moment treat ϕ as being real. Then for $b^2 > 4ac$ the poles are close to the real axis, with an imaginary piece

$$\mp \frac{\epsilon \hat{j}}{\sqrt{b^2 - 4ac}}. \quad (5.8)$$

Since these are on the same side of the real axis for both terms in square brackets it is clear that the contribution to the integral of these two terms cancels even when the singularities are close to the real axis. Consequently there is no S-matrix equivalence evasion in this case, provided that we keep ϕ real as we take the on-shell limit for external legs.

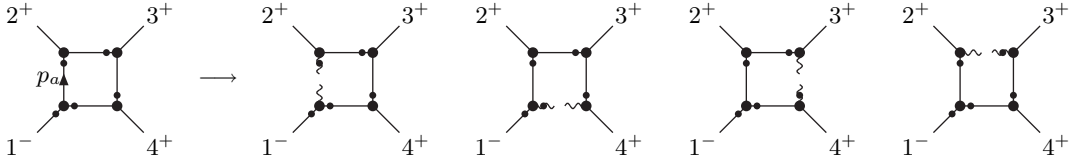
6. One-loop $(-++++)$ amplitude

In [15] we described how the one-loop $(++++)$ amplitude arises in this approach as a tadpole-like diagram constructed from translation kernel. By contrast the one-minus helicity amplitude is constructed from the tadpole diagram of a MHV vertex.

Let us now look at a box diagram, $A(1^-2^+3^+4^+)$ with 1^- attached to MHV $(--++)$ vertex. The integrand of the light-cone amplitude is

$$A^{(1)}(1^-2^+3^+4^+) = 2^4 \frac{V^2(\bar{a}234, 1, a) \bar{V}^2(4, 1a, \bar{a}23) \bar{V}^2(3, 41a, \bar{a}2) \bar{V}^2(2, 341a, \bar{a})}{p_a^2 p_{1a}^2 p_{\bar{a}23}^2 p_{\bar{a}2}^2}. \quad (6.1)$$

It must come from the tadpole diagram in the CSW method by connecting two lines of six-point MHV vertices. We can identify the tadpole contributions to this amplitude in the following way. First, we can cut any one of the four internal lines and get four tree-level MHV diagrams.



MHV vertices are generated by expanding the \mathcal{A} and $\bar{\mathcal{A}}$ in the lagrangian \mathcal{L}^{--++} . We first identify the three point MHV $(--++)$ vertex in the tree-level diagrams and the three parts in the diagrams corresponding to the expansion of \mathcal{A} and $\bar{\mathcal{A}}$ in \mathcal{L}^{--++} . By comparing with the three parts of the diagram, we can find out the corresponding three parts in the light cone amplitude (6.1). Then by replacing the propagators in the light-cone amplitude using (3.17) we can reconstruct the contribution to the one-loop box diagram of the tadpole. The four tree-level diagram contributions are (we label the internal line between leg 1 and 2 as a):

$$A^{(1,1)} = 2^4 \frac{V^2(\bar{a}234, 1, a) \bar{V}^2(4, 1a, \bar{a}23) \bar{V}^2(3, 41a, \bar{a}2) \bar{V}^2(2, 341a, \bar{a})}{p_a^2 \hat{P}_{\bar{a}23} \hat{P}_{\bar{a}2} \hat{P}_{1a} (\frac{P_{1a}^2}{\hat{P}_{1a}} + \frac{P_{\bar{a}}^2}{\hat{P}_{\bar{a}}}) (\frac{P_{41a}^2}{\hat{P}_{41a}} + \frac{P_{\bar{a}}^2}{\hat{P}_{\bar{a}}}) (\frac{P_{341a}^2}{\hat{P}_{341a}} + \frac{P_{\bar{a}}^2}{\hat{P}_{\bar{a}}})}, \quad (6.2)$$

$$A^{(1,2)} = 2^4 \frac{V^2(\bar{a}234, 1, a) \bar{V}^2(4, 1a, \bar{a}23) \bar{V}^2(3, 41a, \bar{a}2) \bar{V}^2(2, 341a, \bar{a})}{P_{1a}^2 \hat{P}_{\bar{a}23} \hat{P}_{\bar{a}2} \hat{P}_{\bar{a}} (\frac{P_{1a}^2}{\hat{P}_{1a}} + \frac{P_{\bar{a}}^2}{\hat{P}_{\bar{a}}}) (\frac{P_{\bar{a}2}^2}{\hat{P}_{\bar{a}2}} + \frac{P_{1a}^2}{\hat{P}_{1a}}) (\frac{P_{\bar{a}23}^2}{\hat{P}_{\bar{a}23}} + \frac{P_{1a}^2}{\hat{P}_{1a}})}, \quad (6.3)$$

$$A^{(1,3)} = 2^4 \frac{V^2(\bar{a}234, 1, a) \bar{V}^2(4, 1a, \bar{a}23) \bar{V}^2(3, 41a, \bar{a}2) \bar{V}^2(2, 341a, \bar{a})}{P_{\bar{a}23}^2 \hat{P}_{\bar{a}} \hat{P}_{\bar{a}2} \hat{P}_{1a} (\frac{P_{41a}^2}{\hat{P}_{41a}} + \frac{P_{\bar{a}}^2}{\hat{P}_{\bar{a}}}) (\frac{P_{41a}^2}{\hat{P}_{41a}} + \frac{P_{\bar{a}2}^2}{\hat{P}_{\bar{a}2}}) (\frac{P_{1a}^2}{\hat{P}_{1a}} + \frac{P_{\bar{a}23}^2}{\hat{P}_{\bar{a}23}})}, \quad (6.4)$$

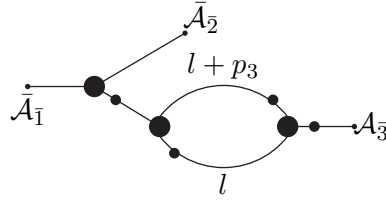
$$A^{(1,4)} = 2^4 \frac{V^2(\bar{a}234, 1, a) \bar{V}^2(4, 1a, \bar{a}23) \bar{V}^2(3, 41a, \bar{a}2) \bar{V}^2(2, 341a, \bar{a})}{P_{341a}^2 \hat{P}_{41a} \hat{P}_{\bar{a}} \hat{P}_{1a} (\frac{P_{1a}^2}{\hat{P}_{1a}} + \frac{P_{\bar{a}2}^2}{\hat{P}_{\bar{a}2}}) (\frac{P_{41a}^2}{\hat{P}_{41a}} + \frac{P_{\bar{a}2}^2}{\hat{P}_{\bar{a}2}}) (\frac{P_{341a}^2}{\hat{P}_{341a}} + \frac{P_{\bar{a}}^2}{\hat{P}_{\bar{a}}})}. \quad (6.5)$$

We have already set the p_i^2 in the denominator of the external particles to zero, since there is no singularity when we put the external particles on-shell. It makes no difference if we take the on-shell limit before or after the LSZ procedure. It is easy to check that these four terms add up to the integrand of the light-cone amplitude for the box diagram (6.1). The other box diagrams, triangle, bubble diagrams of light-cone amplitude can be checked in the same way. There are some subtle problems with diagrams including corrections to

external propagators which we will address in next section. So, in general, one can believe that the one loop one-minus helicity amplitudes should all come just from the tadpoles of MHV vertices.

7. One-loop $(++-)$ amplitude with external tadpole dressing propagators

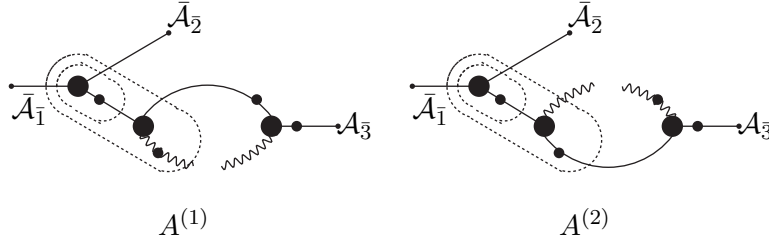
At first sight, for three point $(++-)$ amplitude, there could also be contributions to the cut diagrams considered in the previous section from translation kernels with dressed external propagators, since they yield contributions proportional to tree-level amplitudes which are not zero in $(++-)$ signature. This seems to count diagrams with corrections to external propagators twice. This problem arises from the order of limits in LSZ procedure. In the example of the previous section it does not matter when we take the on shell limit because no singularities are encountered in this limit. But we must be more careful with the diagrams with dressed propagators on external legs because there will then be singularities from $1/\sum \Omega$. We should first calculate the off-shell Green function and then apply the LSZ procedure. Also from the discussion in section (5.2.1) the Green function receives contributions should not just from tadpoles of MHV five point vertices, but also from translation kernels with dressed propagators. Let us look at the example of a light-cone diagram for $\langle \bar{\mathcal{A}}_1 \bar{\mathcal{A}}_2 \mathcal{A}_3 \rangle$:



The integrand of the light-cone computation of the diagram for the Green function is

$$A(1^+ 2^+ 3^-) = ig^6 \frac{\bar{V}^2(1, 2, 3) \bar{V}^2(\bar{3}, l + p_3, \bar{l}) V^2(-l - p_3, 3, l)}{p_1^2 p_2^2 (p_3^2)^2 l^2 (l + p_3)^2}. \quad (7.1)$$

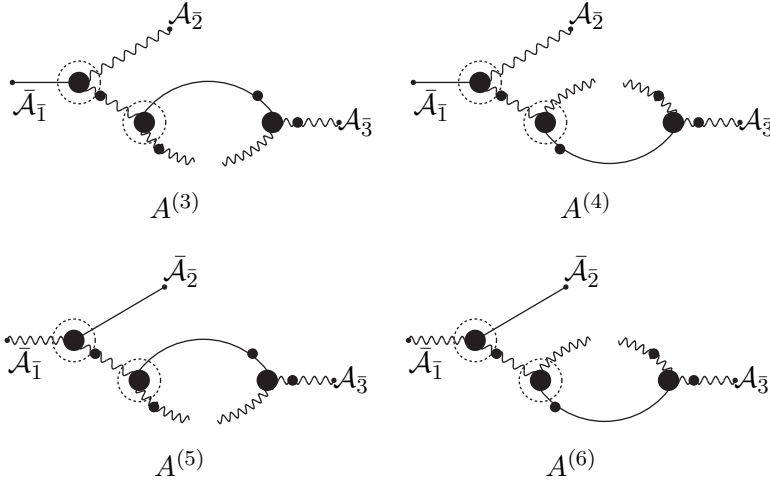
We have omitted the $i\epsilon$ in the propagators. According to the method of the last section, the contribution from the tadpole of MHV five-point vertices to this diagram can be constructed by replacing the corresponding $1/p^2 \rightarrow -1/(2\hat{p} \sum \Omega)$:



$$A^{(1)} = ig^6 \frac{\bar{V}^2(1, 2, 3) \bar{V}^2(\bar{3}, l + p_3, \bar{l}) V^2(-l - p_3, 3, l)}{p_1^2 p_2^2 p_3^2 \hat{3} \left(\frac{p_1^2}{1} + \frac{p_2^2}{2} + \frac{p_3^2}{3} \right) (\hat{l} + \hat{3}) \left(\frac{(l+p_3)^2}{l+3} - \frac{l^2}{l} + \frac{p_1^2}{1} + \frac{p_2^2}{2} \right) l^2}, \quad (7.2)$$

$$A^{(2)} = ig^6 \frac{\bar{V}^2(1, 2, 3) \bar{V}^2(\bar{3}, l + p_3, \bar{l}) V^2(-l - p_3, 3, l)}{p_1^2 p_2^2 p_3^2 \hat{3} \left(\frac{p_1^2}{1} + \frac{p_2^2}{2} + \frac{p_3^2}{3} \right) (-\hat{l}) \left(\frac{(l+p_3)^2}{l+3} - \frac{l^2}{l} + \frac{p_1^2}{1} + \frac{p_2^2}{2} \right) (l + p_3)^2}. \quad (7.3)$$

The contribution from translation kernels with dressed propagators can be represented as four diagrams:



$$A^{(3)} = ig^6 \frac{\bar{V}^2(1, 2, 3) \bar{V}^2(\bar{3}, l + p_3, \bar{l}) V^2(-l - p_3, 3, l)}{p_2^2 (p_3^2)^2 \hat{1} \left(\frac{p_1^2}{1} + \frac{p_2^2}{2} + \frac{p_3^2}{3} \right) (\hat{l} + \hat{3}) \left(\frac{(l+p_3)^2}{l+3} - \frac{l^2}{l} - \frac{p_3^2}{3} \right) l^2}, \quad (7.4)$$

$$A^{(4)} = ig^6 \frac{\bar{V}^2(1, 2, 3) \bar{V}^2(\bar{3}, l + p_3, \bar{l}) V^2(-l - p_3, 3, l)}{p_2^2 (p_3^2)^2 \hat{1} \left(\frac{p_1^2}{1} + \frac{p_2^2}{2} + \frac{p_3^2}{3} \right) (-\hat{l}) \left(\frac{(l+p_3)^2}{l+3} - \frac{l^2}{l} - \frac{p_3^2}{3} \right) (l + p_3)^2}, \quad (7.5)$$

$$A^{(5)} = ig^6 \frac{\bar{V}^2(1, 2, 3) \bar{V}^2(\bar{3}, l + p_3, \bar{l}) V^2(-l - p_3, 3, l)}{p_1^2 (p_3^2)^2 \hat{2} \left(\frac{p_1^2}{1} + \frac{p_2^2}{2} + \frac{p_3^2}{3} \right) (\hat{l} + \hat{3}) \left(\frac{(l+p_3)^2}{l+3} - \frac{l^2}{l} - \frac{p_3^2}{3} \right) l^2}, \quad (7.6)$$

$$A^{(6)} = ig^6 \frac{\bar{V}^2(1, 2, 3) \bar{V}^2(\bar{3}, l + p_3, \bar{l}) V^2(-l - p_3, 3, l)}{p_1^2 (p_3^2)^2 \hat{2} \left(\frac{p_1^2}{1} + \frac{p_2^2}{2} + \frac{p_3^2}{3} \right) (-\hat{l}) \left(\frac{(l+p_3)^2}{l+3} - \frac{l^2}{l} - \frac{p_3^2}{3} \right) (l + p_3)^2}. \quad (7.7)$$

After summing over $A^{(1)}$ to $A^{(6)}$ one finds that the factor $p_1^2/\hat{1} + p_2^2/\hat{2} + p_3^2/\hat{3}$ in the denominator is cancelled and we can apply the LSZ procedure:

$$\begin{aligned} & \lim_{p_1^2, p_2^2, p_3^2 \rightarrow 0} (p_1^2 p_2^2 p_3^2) \int d^4 l \sum_{i=1}^6 A^{(i)} \\ &= \lim_{p_1^2, p_2^2, p_3^2 \rightarrow 0} ig^6 \frac{1}{p_3^2} \int d^4 l \frac{\bar{V}^2(1, 2, 3) \bar{V}^2(\bar{3}, l + p_3, \bar{l}) V^2(-l - p_3, 3, l)}{l^2 (l + p_3)^2} \\ & \quad \times \frac{\left(\frac{(l+p_3)^2}{l+3} - \frac{l^2}{l} + \frac{p_1^2}{1} + \frac{p_2^2}{2} - \frac{p_3^2}{3} \right) \left(\frac{(l+p_3)^2}{l+3} - \frac{l^2}{l} \right)}{\left(\frac{(l+p_3)^2}{l+3} - \frac{l^2}{l} - \frac{p_3^2}{3} \right) \left(\frac{(l+p_3)^2}{l+3} - \frac{l^2}{l} + \frac{p_1^2}{1} + \frac{p_2^2}{2} \right)} \\ &= \lim_{p_1^2, p_2^2, p_3^2 \rightarrow 0} ig^6 \frac{f(p_1^2, p_2^2, p_3^2)}{p_3^2} \\ &= \lim_{p_1^2, p_2^2, p_3^2 \rightarrow 0} ig^6 \frac{\partial f(p_1^2, p_2^2, p_3^2)}{\partial p_3^2}. \end{aligned} \quad (7.8)$$

Since the integration is uniformly convergent after regularization, we can take the limit before integration and differentiation which will give the same on-shell integral as the

light-cone calculation. So we have reproduced the light-cone computation. For the other diagrams with dressed propagators a similar situation happens and it can be checked that they give the same amplitudes as light-cone calculations.

From this example, we see that we should first collect the diagrams with the same internal helicity configurations and with tadpoles on the same legs and then impose the limit $p_1^2, p_2^2, p_3^2 \rightarrow 0$ in the LSZ procedure. Just like at the tree-level, we can also change the order of limits. Because we should take the p_3^2 at the last step after integration, we choose the limit $p_1^2, p_2^2 \rightarrow 0$ first. Then we find that after we multiply $p_1^2 p_2^2 p_3^2$ and take $p_1^2, p_2^2 \rightarrow 0$, the translation kernel contributions from (7.4)–(7.7) vanish and the whole contribution to the amplitude comes from the tadpole of MHV vertices (7.2)–(7.3). The $p_1^2/\hat{1} + p_2^2/\hat{2} + p_3^2/\hat{3}$ simply contributes to the propagator i/p_3^2 needed in the amplitude. So the result is that we do not need to consider the translation kernel contribution in this case.

In section 5.2.1, we have argued that since the sum of one-loop diagrams in which the external legs are dressed are proportional to tree-level amplitudes, their contributions to higher point one-minus-helicity amplitudes vanish. But it is also instructive to apply the above arguments to these higher point amplitudes. In fact, a similar situation occurs. For these amplitudes there are also $1/(\sum_i p_i^2/\hat{i})$ factors both from the tadpoles of MHV vertices and the translation kernels, where i enumerates all the external momenta. If we collect the diagrams with the same internal helicity configuration and with tadpoles on the same legs first, (including tadpoles of MHV vertices and translation kernels,) then the $\sum_i p_i^2/\hat{i}$ in the denominator is cancelled and we can take the on-shell limits in any order. If we first set all the external legs on-shell except that with the tadpole then the translation kernel contributions vanish leaving just the tadpoles of MHV vertices. So we come to the conclusion that we do not need to consider external propagators dressed by tadpoles from translation kernel.

8. Conclusion and higher loops

We have seen that the S-matrix equivalence theorem is not immediately applicable to the change of variables from \mathcal{A} and $\bar{\mathcal{A}}$ to \mathcal{B} and $\bar{\mathcal{B}}$ because of the non-locality of the translation kernels, and this accounts for the one-loop all plus helicity amplitudes apparently missing from the CSW rules. However, by analysing the mechanisms that generate singularities in the external momenta that are able to cancel the LSZ factors we have seen that the types of amplitude in which S-matrix equivalence is violated are very restricted. At tree-level the amplitudes that might have displayed this violation actually vanish. At one-loop the equivalence violating amplitudes that do not vanish are ones in which all the gluons have positive helicity, and these have a known form, e.g. (2.1). Because the only non-zero one-loop amplitudes that show S-matrix equivalence violation are given by the tadpole diagrams in which the single $\bar{\mathcal{B}}$ field of an $\bar{\mathcal{A}}$ translation kernel is contracted with a \mathcal{B} field it follows that higher loops can only contribute to violating processes by dressing the legs of these one-loop diagrams. So, apart from this class of known amplitudes we are free to calculate S-matrix elements using the \mathcal{B} and $\bar{\mathcal{B}}$ fields directly.

Since one-minus-helicity diagrams can not be constructed from more than one MHV vertex or from completion vertices, they can only arise as tadpoles of MHV vertices. By analysing an example we saw how the light-cone amplitudes really can be reconstructed from tadpoles of MHV vertices.

We found a new recursion relation for the expansion coefficients Ξ^s of $\bar{\mathcal{A}}$, which encoded a cancellation of certain singularities that would otherwise have contributed to further evasion of the S-matrix equivalence theorem. Using this recursion relation for Ξ together with the one for Υ we were led to a better understanding of the canonical transformation: they can be reconstructed from the light-cone tree level diagrams built with only $(+ + -)$ vertices by replacing the propagator using (3.17). This was useful in discussing the relationship between light-cone and MHV methods.

A few remarks about the rational parts of one-loop diagrams is in order. The CSW or MHV rules, although initially conjectured and proven at tree-level have been studied at one-loop level. It has been shown that they give supersymmetric amplitudes correctly [13, 24, 25, 26], but when applied to non-supersymmetric amplitudes, the rational parts can not be correctly reproduced [27], not only in all-plus diagrams. Our discussion in the present paper has focussed on the (limited) breakdown of the equivalence theorem that is responsible, in our approach, for the rational one-loop all plus amplitude in non-supersymmetric Yang-Mills. Our conclusion is that only these amplitudes require the use of the translation kernels, and so all other one-loop amplitudes can be calculated directly from the Green functions of the B fields. One may then ask where the missing rational parts of the other diagrams might come from. Here, we should point out that we have formulated the transformation from light-cone Yang-Mills to the new MHV Lagrangian in D dimensions. Consequently our canonical transformation coefficients Υ and Ξ are formulated in D dimensions ($D = 4 - 2\epsilon$) and the MHV vertices derived from these coefficients are also in D dimensions, whether one uses standard dimensional regularisation as in [15] or FDH. This is different from the usual analyses of MHV one-loop calculations in [13, 24, 25, 26, 27] which use four dimensional MHV vertices. In the FDH procedure the ϵ dependence enters the transformation coefficients only through $\sum \Omega = \sum p^2/\hat{p}$ where p^2 is the D -dimensional momentum, rather than the four dimensional momentum, in recursion relations (3.5) and (3.9), but this is enough to make the vertices of our Lagrangian different from the ordinary four dimensional Parke-Taylor vertices. In ordinary dimensional regularisation the vertices would, in addition, acquire indices relating to the extra dimensions. In either formalism the vertices differ from the four dimensional ones. One would expect that, in general, these modifications would produce terms proportional to ϵ which would cancel the divergence $1/\epsilon$ from the loop integration resulting in rational pieces missing in the ordinary MHV calculation.

Our arguments can easily be extended to super Yang-Mills theory using the supersymmetry transformation in [28]. We expect the supersymmetry transformation is not affected in D dimensions, and the results in [28] can be directly used here after setting the chiral fields to zero. The \mathcal{A} transformation is not changed. From equation (B.7) and (C.14) in

[28], $\bar{\mathcal{A}}$ has an additional term which involves gluino Π :

$$\bar{\mathcal{A}}_q^{B\Pi} = -\frac{1}{\sqrt{2}\hat{q}} \sum_{n=2}^{\infty} \int_{1\dots n} \sum_{s=1}^n \left[\Xi_{q,\bar{1}\dots\bar{n}}^s \sum_{l=1, l\neq s}^n (-1)^{\delta_{ls}} \mathcal{B}_1 \dots \Pi_l \dots \bar{\Pi}_s \dots \mathcal{B}_n \right] \delta_{q\bar{1}\dots\bar{n}}, \quad (8.1)$$

Ξ^s is just the coefficient appearing in the pure bosonic expansion. The fermion propagator and bosonic propagators are

$$\langle \Pi \bar{\Pi} \rangle = \frac{i g^2 \hat{p}}{\sqrt{2} p^2}, \quad \langle \mathcal{A} \bar{\mathcal{A}} \rangle = \frac{i g^2}{2 p^2}. \quad (8.2)$$

Considering the $\sqrt{2}\hat{p}$ factor, when connected to a gluino propagator the coefficient is the same as the one in the pure bosonic expansion up to a sign. So all the foregoing discussion can be applied to diagrams with inner gluinos. Therefore one would expect that only the tadpole would evade the equivalence theorem. One can easily check that the all-plus translation kernel contribution to the amplitude is cancelled using above expansion (8.1). We also expect that our MHV calculation should reproduce the light-cone super Yang-Mills calculation, so the one-minus-helicity amplitude in supersymmetric Yang-Mills should also be zero. As is well known [21], in supersymmetric theories the rational parts of amplitudes are determined uniquely by their (four dimensional) cut-constructible parts. It follows that all the remaining rational parts discussed in the previous paragraph should be cancelled in the supersymmetric theory.

Acknowledgements

Tim, Xiao, and Paul thank STFC for support under the rolling grants ST/G000557/1 and ST/G000433/1, and Jonathan thanks the Richard Newitt bursary scheme, for financial support. It is a pleasure to acknowledge useful conversations with James Eittle.

A. Some remaining thoughts on translation kernels

The careful reader may have noticed that the translation kernel can become ill-defined due to the symmetry of graphs. For instance in the tadpole graph below arising from self-contraction of the $\Xi^2 \bar{\mathcal{B}} \mathcal{B} \mathcal{B}$ term the gluons flowing in and out of the kernel must carry equal and opposite momenta as required by conservation of momentum. As a result the factors $(p_j^2 + i\epsilon)/\hat{p}_j$ which appear in the denominator of the kernel cancel in pairs. The same cancellation can also occur for special values of momentum. Note that in this case the standard $i\epsilon$ prescription fails to prevent $\sum(p_j^2 + i\epsilon)/\hat{p}_j$ from vanishing.

This problem can be fixed by adding a small correction to the definition of translation kernels. To break symmetry we distinguish the $i\epsilon$ associated with \mathcal{A} fields and \mathcal{B} fields. $\Upsilon(123)$ is now modified as

$$\Upsilon(123) = \frac{i \left(\frac{\bar{p}_2}{\hat{p}_2} - \frac{\bar{p}_3}{\hat{p}_3} \right)}{\frac{p_1^2 + i\epsilon_A}{\hat{p}_1} + \frac{p_2^2 + i\epsilon_B}{\hat{p}_2} + \frac{p_3^2 + i\epsilon_B}{\hat{p}_3}} \quad (A.1)$$

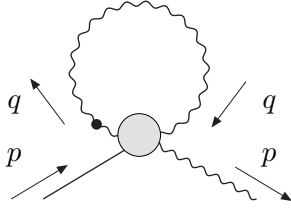


Figure 1: Translation kernels diverge in symmetrical graphs

Higher order terms in the \mathcal{A} field expansion can all be redefined following the same spirit and the coefficients for the $\bar{\mathcal{A}}$ expansion are in turn determined from the canonical transformation condition (3.8). However a small price is to be paid for getting around the divergences. By substituting the modified kernels back into (1.7) which used to define Υ we find two sides of the equation slightly mismatch. The differences generate new vertices carrying infinitesimal corrections.

$$\frac{p^2 + i\epsilon_A}{\hat{p}} A(p) + i \int d^{D-1} q \left[\frac{\bar{q}}{\hat{q}} A(q), A(p-q) \right] \quad (\text{A.2})$$

$$= \int d^{D-1} q \frac{q^2 + i\epsilon_A}{\hat{q}} B(q) \frac{\delta A(p)}{\delta B(q)} + \sum_{n=2}^{\infty} \int \left(\prod_{i=2}^n d^{D-1} q_{(i)} \right) \left(\sum_{j=2}^n \frac{i(\epsilon_A - \epsilon_B)}{\hat{q}_j} \right) \Upsilon_{12\dots n} B(q_2) \dots B(q_n) \quad (\text{A.3})$$

$$= \int d^{D-1} q \frac{q^2 + i\epsilon_A}{\hat{q}} B(q) \frac{\delta A(p)}{\delta B(q)} + \frac{i(\epsilon_A - \epsilon_B)}{\hat{q}} B(q) \frac{\delta A(p)}{\delta B(q)} - \frac{i(\epsilon_A - \epsilon_B)}{\hat{p}} B(p) \quad (\text{A.4})$$

Equivalently this can be written as

$$\mathcal{L}^{-+}[\mathcal{A}, \bar{\mathcal{A}}] + \mathcal{L}^{-++}[\mathcal{A}, \bar{\mathcal{A}}] = \mathcal{L}^{-+}[\mathcal{B}, \bar{\mathcal{B}}] + \mathcal{L}_{\epsilon}[\mathcal{B}, \bar{\mathcal{B}}] \quad (\text{A.5})$$

where \mathcal{L}_{ϵ} represents the new vertex terms.

$$\begin{aligned} \mathcal{L}_{\epsilon}[\mathcal{B}, \bar{\mathcal{B}}] &= -\bar{\mathcal{A}} i(\epsilon_A - \epsilon_B) \mathcal{B} + \bar{\mathcal{B}}(\epsilon_A - \epsilon_B) \mathcal{B} \\ &= \left(\sum_{m=2}^{\infty} \sum_{s=2}^m \int_{2\dots m} \frac{\hat{s}}{\hat{p}} \Xi^{s-1} \mathcal{B} \dots \bar{\mathcal{B}} \dots \mathcal{B} \right) i(\epsilon_A - \epsilon_B) \mathcal{B} \end{aligned} \quad (\text{A.6})$$

Introducing double circles to denote the factor $\frac{\hat{s}}{\hat{p}} i(\epsilon_A - \epsilon_B)$, these terms are expressed graphically as

In most cases these corrections do not really enter into our calculations because of the infinitesimal nature of the vertices, except for extremely divergent graphs such as (Fig.1). Because of the asymmetry treatment the factor $\sum(p_j^2 + i\epsilon)/\hat{p}_j$ in the denominator of the kernel do not cancel completely. A factor of $i(\epsilon_A - \epsilon_B)/\hat{p}$ in the translation kernel is left to cancel the infinitesimal factor brought by the new vertex, resulting a finite contribution to the loop integral. It is straightforward to show the following four graphs (Fig.3(a) to

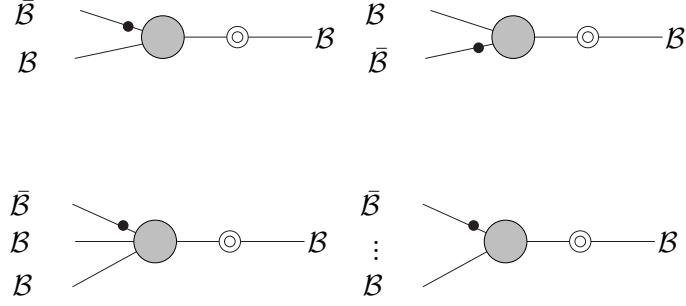


Figure 2: Infinitesimal vertex terms

Fig.3(d)) constructed from the new vertex restore the $\langle \bar{\mathcal{A}}\bar{\mathcal{A}} \rangle$ self-energy bubble integral in the LCYM theory (Fig.4(a)).

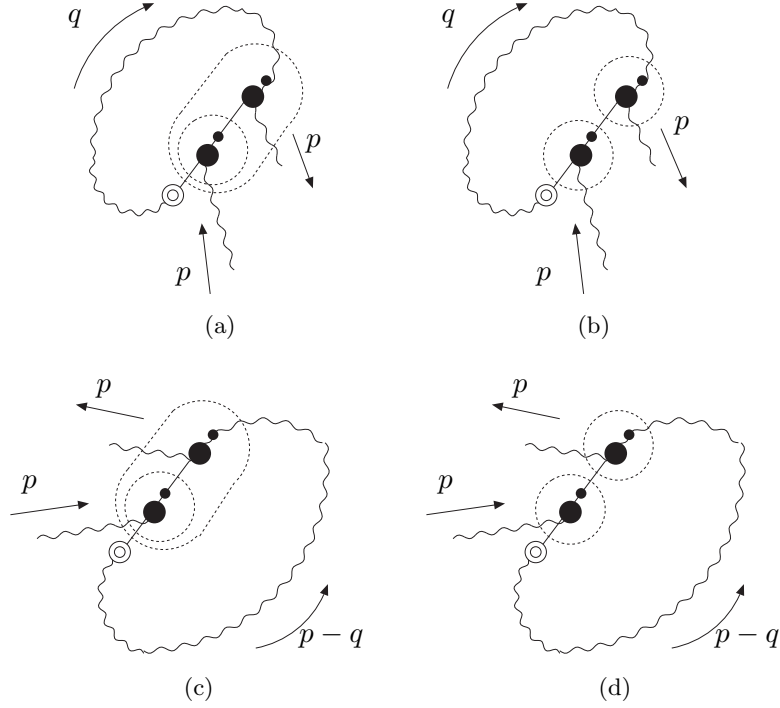


Figure 3: Contributions to the $\langle \bar{\mathcal{A}}\bar{\mathcal{A}} \rangle$ symmetric loop graph

$$\bar{\mathcal{A}} \text{---} + \begin{array}{c} + \quad - \\ - \quad + \end{array} \text{---} \bar{\mathcal{A}}$$

Figure 4: $\langle \bar{\mathcal{A}}\bar{\mathcal{A}} \rangle$ self-energy graph in the LCYM theory

Another issue regarding $i\epsilon$ prescription arises if we wish to apply (3.12) to simplify $\bar{\mathcal{A}}$ expansions. In the example illustrated below (Fig.5) the first two graphs are combined according to the identity (A.7).

$$\begin{aligned}
& \frac{1}{\frac{p_3^2+i\epsilon_B}{\hat{p}_3} + \frac{p_4^2+i\epsilon_A}{\hat{p}_4} + \frac{(p_1+p_2)^2+i\epsilon_B}{\hat{p}_1+\hat{p}_2}} - \frac{1}{\frac{p_1^2+i\epsilon_B}{\hat{p}_1} + \frac{p_2^2+i\epsilon_B}{\hat{p}_2} + \frac{p_3^2+i\epsilon_B}{\hat{p}_3} + \frac{p_4^2+i\epsilon_A}{\hat{p}_4}} \\
&= \frac{1}{\frac{p_3^2+i\epsilon_B}{\hat{p}_3} + \frac{p_4^2+i\epsilon_A}{\hat{p}_4} + \frac{(p_1+p_2)^2+i\epsilon_B}{\hat{p}_1+\hat{p}_2}} \frac{\frac{p_1^2+i\epsilon_B}{\hat{p}_1} + \frac{p_2^2+i\epsilon_B}{\hat{p}_2} + \frac{(p_3+p_4)^2+i\epsilon_B}{\hat{p}_3+\hat{p}_4}}{\frac{p_1^2+i\epsilon_B}{\hat{p}_1} + \frac{p_2^2+i\epsilon_B}{\hat{p}_2} + \frac{p_3^2+i\epsilon_B}{\hat{p}_3} + \frac{p_4^2+i\epsilon_A}{\hat{p}_4}} \quad (\text{A.7})
\end{aligned}$$

Figure 5: Simplification of the $\bar{\mathcal{A}}$ expansion

However we see in (A.7) the numerator generated from subtraction has a different $i\epsilon$ associated with line (p_3+p_4) and does not exactly cancel the factor $1/\left(\frac{p_1^2+i\epsilon_B}{\hat{p}_1} + \frac{p_2^2+i\epsilon_B}{\hat{p}_2} + \frac{(p_3+p_4)^2+i\epsilon_A}{\hat{p}_3+\hat{p}_4}\right)$ represented by the small dash line circle on the left. The difference can be accounted for if we introduce even more correction graphs carrying infinitesimal vertices.

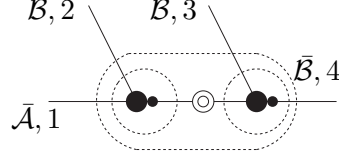
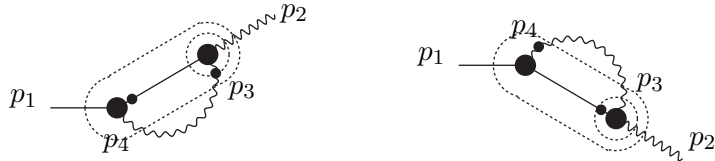


Figure 6: Correction term to the $\bar{\mathcal{A}}$ expansion

$$\begin{aligned} & \frac{i(\epsilon_A - \epsilon_B)}{\hat{p}_3 + \hat{p}_4} \frac{1}{\frac{p_3^2+i\epsilon_B}{\hat{p}_3} + \frac{p_4^2+i\epsilon_A}{\hat{p}_4} + \frac{(p_1+p_2)^2+i\epsilon_B}{\hat{p}_1+\hat{p}_2}} \\ & \times \frac{1}{\frac{p_1^2+i\epsilon_B}{\hat{p}_1} + \frac{p_2^2+i\epsilon_B}{\hat{p}_2} + \frac{(p_3+p_4)^2+i\epsilon_A}{\hat{p}_3+\hat{p}_4}} \frac{1}{\frac{p_1^2+i\epsilon_B}{\hat{p}_1} + \frac{p_2^2+i\epsilon_B}{\hat{p}_2} + \frac{p_3^2+i\epsilon_B}{\hat{p}_3} + \frac{p_4^2+i\epsilon_A}{\hat{p}_4}} \end{aligned} \quad (\text{A.8})$$

Again these corrections can generally be neglected except for symmetrical tadpoles such as the graph constructed by contracting leg p_3 and p_4 .

Another way to deal with this problem without bothering with the $i\epsilon$ is to change the orders of the LSZ procedure and the overall delta function. Let us look at diagrams:



We can impose $\delta(\hat{p}_1 + \hat{p}_2)$ and the momentum conservation on the right vertex, then apply LSZ procedure and impose the $\delta(\bar{p}_1 + \bar{p}_2)\delta(\tilde{p}_1 + \tilde{p}_2)$ at last. In the LSZ procedure we impose

$$\bar{1} \text{---} \textcircled{2} \begin{matrix} \nearrow \bar{2} \\ \searrow \bar{3} \end{matrix} = - \bar{1} \text{---} \textcircled{2} \bullet \text{---} \bar{3} = \text{---} \textcircled{\bullet} \begin{matrix} \nearrow \\ \searrow \end{matrix} .$$

For $n = 4$, $\Xi^1(\bar{1}\bar{2}\bar{3}\bar{4})$:

$$\bar{1} \text{---} \textcircled{3} \begin{matrix} \nearrow \bar{2} \\ \searrow \bar{4} \end{matrix} = - \left[\text{---} \textcircled{2} \bullet \textcircled{2} \begin{matrix} \nearrow \\ \searrow \end{matrix} + \text{---} \textcircled{3} \bullet \text{---} \right] \quad (\text{B.2})$$

$$= - \left[\text{---} \textcircled{2} \bullet \textcircled{2} \begin{matrix} \nearrow \\ \searrow \end{matrix} - \left[\text{---} \textcircled{2} \bullet \bullet \text{---} + \text{---} \textcircled{2} \bullet \bullet \text{---} \right] \right] \quad (\text{B.3})$$

$$= - \left[\text{---} \textcircled{\bullet} \bullet \textcircled{2} \begin{matrix} \nearrow \\ \searrow \end{matrix} - \text{---} \textcircled{2} \bullet \bullet \text{---} \right] \quad (\text{B.4})$$

$$= \text{---} \textcircled{\bullet} \bullet \textcircled{2} \begin{matrix} \nearrow \\ \searrow \end{matrix} + \text{---} \textcircled{2} \bullet \bullet \text{---} . \quad (\text{B.5})$$

Equation (B.2) is just the old recursion relation. From (B.2) to (B.3) we expand the second term. From (B.3) to (B.4) we combine the first two terms using (3.11). Then the recursion relation for $\Xi^1(\bar{1}\bar{2}\bar{3}\bar{4})$ is proven. Similarly, one can also prove that $\Xi^2(\bar{1}\bar{2}\bar{3}\bar{4})$, $\Xi^3(\bar{1}\bar{2}\bar{3}\bar{4})$ satisfy the recursion relation.

For Ξ^s with general n arguments, we suppose that for Ξ^s with less than n arguments the recursion relation is already proven. Then at the first step we combine the following terms from the old recursion relation

$$- \left[\bar{1} \text{---} \textcircled{n-2} \bullet \textcircled{2} \begin{matrix} \nearrow \bar{i-1} \\ \searrow \bar{i} \end{matrix} + \bar{1} \text{---} \textcircled{n-2} \bullet \textcircled{2} \begin{matrix} \nearrow \bar{i} \\ \searrow \bar{i+1} \end{matrix} + \bar{1} \text{---} \textcircled{n-1} \bullet \text{---} \right] . \quad (\text{B.6})$$

By expanding the third term using recursion for Υ and combining terms, using the relation

(3.11), we obtain

$$\begin{aligned}
& \text{Diagram 1} + \text{Diagram 2} + \sum_{m \geq 2} \text{Diagram 3} \\
& + \sum_{m \geq 2} \text{Diagram 4}
\end{aligned}
\tag{B.7}$$

The diagrams are Feynman-like diagrams with external lines and internal blobs. Diagram 1 and 2 show a black blob connected to a grey blob labeled 2, with external lines labeled $\bar{i}-1$, \bar{i} , and $\bar{i}+1$. Diagram 3 shows a white blob connected to a black blob connected to a grey blob labeled m , with external lines labeled \bar{i} and \bar{l} . Diagram 4 is similar to Diagram 3 but with a different internal structure.

The first two terms come from the first two terms in (B.6) combined with two terms from the expansion of the last terms in (B.6). The two sums are what is left from the expansion of the last term in (B.6).

For step $l-1$, $3 \leq l \leq n-3$, we combine terms

$$\begin{aligned}
& - \left[\sum \text{Diagram 5} - \sum \text{Diagram 6} - \sum_{m \geq 2} \text{Diagram 7} \right. \\
& \left. - \sum_{m \geq 2} \text{Diagram 8} \right]
\end{aligned}
\tag{B.8}$$

The diagrams are Feynman-like diagrams. Diagram 5 shows a white blob connected to a grey blob labeled l , with external lines labeled \bar{i} and \bar{l} . Diagram 6 shows a black blob connected to a grey blob labeled $l-1$, with external lines labeled \bar{i} and \bar{l} . Diagram 7 and 8 show more complex structures with multiple blobs and external lines.

where the first term is from the old recursion relation, the second term and the $m = 2$ terms in the last two sums come from step $l-2$ and the other terms in the sums come from step $l-m$. After expanding the grey blob in the first term and the black blob in the second terms, collecting terms using the relation (3.11) and counting in the other terms left from step $l-m$, we obtain

$$\sum \text{Diagram 9} + \sum_{m \geq 1} \sum_{r \geq m+1} \left[\text{Diagram 10} + \text{Diagram 11} \right].
\tag{B.9}$$

The diagrams are Feynman-like diagrams. Diagram 9 shows a black blob connected to a grey blob labeled l , with external lines labeled \bar{i} and \bar{l} . Diagram 10 and 11 show more complex structures with multiple blobs and external lines.

Iterate this procedure from (B.8), and at the last step $l = n-2$, one can find the result (B.9) is just the right hand side of the recursion relation to be proved.

References

- [1] F. Cachazo, P. Svrcek and E. Witten, JHEP **0409**, 006 (2004) [arXiv:hep-th/0403047].

- [2] E. Witten, Commun. Math. Phys. **252** (2004) 189 [arXiv:hep-th/0312171].
- [3] R. Britto, F. Cachazo, B. Feng and E. Witten, Phys. Rev. Lett. **94** (2005) 181602 [arXiv:hep-th/0501052].
- [4] R. Boels, L. Mason and D. Skinner, JHEP **0702** (2007) 014 [arXiv:hep-th/0604040].
- [5] L. J. Mason and D. Skinner, Phys. Lett. B **636** (2006) 60 [arXiv:hep-th/0510262].
- [6] R. Boels, L. Mason and D. Skinner, Phys. Lett. B **648** (2007) 90 [arXiv:hep-th/0702035].
- [7] R. Boels, Phys. Rev. D **76** (2007) 105027 [arXiv:hep-th/0703080].
- [8] R. Boels, C. Schwinn and S. Weinzierl, arXiv:0712.3506 [hep-ph].
- [9] R. Boels and C. Schwinn, JHEP **0807** (2008) 007 [arXiv:0805.1197 [hep-th]].
- [10] R. Boels and C. Schwinn, arXiv:0805.4577 [hep-th].
- [11] A. Gorsky and A. Rosly, JHEP **0601** (2006) 101 [arXiv:hep-th/0510111].
- [12] P. Mansfield, JHEP **0603** (2006) 037 [arXiv:hep-th/0511264].
- [13] A. Brandhuber, B. J. Spence and G. Travaglini, Nucl. Phys. B **706** (2005) 150 [arXiv:hep-th/0407214].
- [14] G. Chalmers and W. Siegel, Phys. Rev. D **54** (1996) 7628 [arXiv:hep-th/9606061].
- [15] J.H. Eittle, C.-H. Fu, J.P. Fudger, P.R. W. Mansfield, and T.R. Morris, JHEP **0705**, 011 (2007) [arXiv:hep-th/0703286].
- [16] J. H. Eittle and T. R. Morris, JHEP **0608**, 003 (2006) [arXiv:hep-th/0605121].
- [17] S. J. Parke and T. R. Taylor, Phys. Rev. Lett. **56** (1986) 2459.
- [18] W. A. Bardeen, Prog. Theor. Phys. Suppl. **123** (1996) 1.
- [19] Z. Bern and D. A. Kosower, Nucl. Phys. B **379** (1992) 451.
- [20] Z. Bern and A. G. Morgan, Nucl. Phys. B **467** (1996) 479 [arXiv:hep-ph/9511336].
- [21] Z. Bern, L. J. Dixon, D. C. Dunbar and D. A. Kosower, Nucl. Phys. B **435** (1995) 59 [arXiv:hep-ph/9409265].
- [22] Wen Jiang, D.Phil Thesis. Oxford University, 2008.
- [23] A. Brandhuber, B. Spence, G. Travaglini and K. Zoubos, JHEP **0707** (2007) 002 [arXiv:0704.0245 [hep-th]].
- [24] C. Quigley and M. Rozali, JHEP **0501** (2005) 053 [arXiv:hep-th/0410278].
- [25] J. Bedford, A. Brandhuber, B. J. Spence and G. Travaglini, Nucl. Phys. B **706** (2005) 100 [arXiv:hep-th/0410280].
- [26] A. Brandhuber, B. Spence and G. Travaglini, JHEP **0601** (2006) 142 [arXiv:hep-th/0510253].
- [27] J. Bedford, A. Brandhuber, B. J. Spence and G. Travaglini, Nucl. Phys. B **712** (2005) 59 [arXiv:hep-th/0412108].
- [28] T. R. Morris and Z. Xiao, JHEP **0812** (2008) 028 [arXiv:0810.3684 [hep-th]].